

Centre Eau Terre Environnement

MODÉLISATION DE LA VARIABILITÉ INTER ANNUELLE ET DE L'ÉVOLUTION DE LA VITESSE DU VENT EN ONTARIO

Par

Khaoula Laazibi

Mémoire présenté pour l'obtention du grade de
Maître ès Sciences (M. Sc.)
en sciences de la terre

Jury d'évaluation

Président du jury et
examinateur interne

André St-Hilaire
INRS

Examinateur externe

Jeannine-Marie St-Jacques
Département de Géographie,
Aménagement, Environnement
Université Concordia

Directeur de recherche

Taha B.M.J. Ouarda
INRS

AVANT-PROPOS

Ce mémoire rentre dans le cadre de l'obtention du grade de Maître ès Sciences de la terre. Ce document intitulé « Modélisation de la variabilité interannuelle et de l'évolution de la vitesse du vent » est un mémoire de maîtrise par article scientifique. Le premier chapitre comporte une synthèse qui présente un résumé des méthodes et des résultats. Le deuxième chapitre présente l'article produit.

Titre de l'article: Inter-annual variability and teleconnections of wind speed: a case study in Ontario.

Auteurs : Khaoula Laazibi, Taha B.M.J. Ouarda.

REMERCIEMENTS

Tout d'abord, je tiens à exprimer ma reconnaissance à mon directeur de mémoire, Monsieur Taha Ouarda, Professeur et titulaire de la Chaire de recherche du Canada en hydro-climatologie statistique, pour ses judicieux conseils professionnels et surtout pour avoir contribué à alimenter et guider mes réflexions. Je remercie également tous les professeurs intervenant dans ma formation et les membres de mon jury.

Je tiens à témoigner ma gratitude à ma compagne Wiem Rjeb pour sa confiance et le soutien inestimable qu'elle m'a apporté tout au long de nos travaux. Merci à ma collègue Doctorante et amie Zina Souaissi d'avoir partagé ses connaissances et ses expériences. Elle a été d'un grand soutien et ses conseils était précieux. À titre personnel je remercie ma famille, ma sœur Fatma et mes amies Alice, Ophélie et Nadia pour l'encouragement et le soutien inconditionnel.

Enfin, Je présente mes remerciements à toutes les personnes qui ont contribué de près ou de loin à l'élaboration de ce mémoire de recherche.

RESUME

Les extrêmes du vent doivent être adéquatement estimés afin d'assurer la sécurité des structures et des vies humaines. Une estimation qui ne tient pas compte de la variabilité de la vitesse du vent et des tendances à long terme ou qui est basée sur une courte période d'enregistrement, peut conduire à des conséquences écologiques et socio-économiques néfastes. Il faudra alors analyser les non-stationnarités qui peuvent exister dans les séries temporelles des variables induites par des phénomènes naturels. L'objectif de ce présent mémoire est de dévoiler les modes principaux de la variabilité de la vitesse du vent en Ontario ; et d'étudier les liens de dépendance à l'échelle de corrélation entre les vitesses annuelles et les indices climatiques de basse fréquence. Parmi les variables considérées figurent les vitesses maximales et moyennes annuelles du vent, non seulement pour évaluer le potentiel éolien mais aussi pour assurer la stabilité des structures.

Les approches linéaires ne permettent pas d'aboutir à une représentation adéquate des relations de dépendance complexes entre les variables. L'analyse spectrale en ondelettes, ou « Wavelet Analysis » en anglais, permet d'étudier les processus non stationnaires et d'établir les liens complexes entre les vitesses du vent et les oscillations climatiques dans la zone d'étude.

L'investigation des liens de corrélation a permis de retenir trois indices climatiques dominants dans la zone d'étude ; L'indice de l'Atlantique de l'Est « East Atlantic (EA) », l'Oscillation de l'Atlantique du Nord « North Atlantic Oscillation (NAO) » et l'Oscillation Décennale du Pacifique « Pacific Decadal Oscillation (PDO) ». La transformée continue en ondelettes révèle des non stationnarités et des ruptures dans la majorité des séries de vitesse du vent confirmant les résultats de l'analyse de tendance et des changements au cours du temps. Des zones de cohérences à différentes échelles (interannuelle, décennale et multi-décennale) et persistantes à grande échelle confirment l'impact potentiel des indices climatiques retenus sur la variabilité interannuelle de la vitesse du vent en Ontario.

Variabilité ; vitesse du vent ; téléconnexions ; tendance ; détection des points de changement ; analyse de corrélation ; analyse en ondelettes ; indice climatique ; Ontario.

TABLE DES MATIÈRES

AVANT-PROPOS	III
REMERCIEMENTS	V
RESUME	VI
TABLE DES MATIÈRES	VII
LISTE DES ABRÉVIATIONS.....	IX
CHAPITRE 1 : SYNTHÈSE	2
1 INTRODUCTION.....	4
1.1 PROBLÈME	5
1.2 OBJECTIFS.....	5
1.3 ORIGINALITÉ.....	5
1.4 ORGANISATION DE LA SYNTHÈSE	5
2 ZONE D'ETUDE ET VARIABLES UTILISEES	7
3 MÉTHODES.....	8
3.1 ANALYSE DE TENDANCE À LONG TERME	8
3.2 MÉTHODE BAYÉSIENNE DE DÉTECTION DE MULTIPLES POINTS DE CHANGEMENT.....	8
3.3 ANALYSE DE CORRELATION	9
3.4 ANALYSE SPECTRALE EN ONDELETTES.....	9
4 RÉSULTATS.....	11
5 CONCLUSIONS ET PERSPECTIVE	12
6 RÉFÉRENCES.....	13
CHAPITRE 2: INTER-ANNUAL VARIABILITY AND TELECONNECTIONS OF WIND SPEED: CASE STUDY OF ONTARIO, CANADA	16

LISTE DES ABRÉVIATIONS

AMO: Atlantic Multidecadal Oscillation

AO: Arctic Oscillation

CWT: Continuous Wavelet Transform

EA: East Atlantic

ENSO: El Niño Southern Oscillation

IOD: Indian Ocean Dipole

JFM: January-February-March

NAO: North Atlantic Oscillation

NAOJ: North Atlantic Oscillation (Jones)

NWP: Numerical Weather Prediction

OND: October-November-December

PDO: Pacific Decadal Oscillation

PNA: Pacific North American

SOI: Southern Oscillation Index

TNA: Tropical Northern Atlantic

WA: Wavelet Analysis

WTC: Wavelet Transform Coherence

WHWP: Western Hemisphere warm pool

XWT: Cross Wavelet Transform

CHAPITRE 1 : SYNTHÈSE

1 INTRODUCTION

Le vent est considéré comme l'une des sources d'énergies renouvelables les moins coûteuses et les plus facilement disponibles. Étant donné que la production d'énergie éolienne dépend fortement de la vitesse du vent, la connaissance de la variabilité de celle-ci est nécessaire à l'essor de l'industrie (Burton et al., 2001). Les modèles classiques utilisés pour l'évaluation de l'énergie éolienne ne prennent pas en considération l'influence des schémas de circulation atmosphérique sur la vitesse du vent. Les prévisions à court ou à long terme des indices climatiques à grande échelle peuvent améliorer les modèles d'évolution future de la vitesse du vent et, par conséquent, mieux prédire le potentiel énergétique pendant la durée de vie d'un projet éolien.

Certaines approches ont été proposées pour intégrer les oscillations climatiques dans les outils de prévision de la vitesse ou de la puissance du vent à long terme (Correia et al. 2017, Jerez and Trigo 2013, Naizghi and Ouarda 2016, Ouarda et Charron 2021). Ces oscillations, lorsqu'elles sont considérées, permettent d'aboutir à des modèles de prévision précis. Peu de recherches reconnaissent les effets importants de la variabilité climatique tel que représentée par les indices dans l'Atlantique tropical. Selon Hurrell et Deser (2010), les variations de la circulation atmosphérique influencent de manière significative la variabilité de la vitesse du vent.

Les approches de prévision existantes dans la littérature appliquent soit des modèles autorégressifs, qui extrapolent les vitesses observées dans le futur en utilisant une analyse linéaire ou non linéaire des séries temporelles (Alexiadis et al., 1998), soit des modèles de prédition climatique numérique (Numerical Weather Prediction, NWP) régionaux (méso-échelle) (Landberg, 2001). La première approche n'utilise que les observations passées de la région d'étude considérée, et n'est donc utile que pour les prévisions à court terme. La seconde approche est généralement bien supérieure pour fournir des prévisions au-delà de quelques heures. Néanmoins, l'utilisation des approches non-linéaires pour étudier l'évolution à long terme de la vitesse du vent et ses liens de dépendance à l'échelle de cohérence avec les indices climatiques d'oscillations de basse fréquence n'a jamais été effectuée en Ontario, la province qui domine l'énergie éolienne au Canada.

1.1 PROBLÈME

Les modèles linéaires classiques ne peuvent pas fournir une représentation adéquate de la vitesse du vent, compte tenu de sa nature complexe. Ainsi, ces derniers ne prennent pas en compte les relations de dépendance entre la vitesse du vent et les indices climatiques de basse fréquence. De plus la plupart des modèles de prévision sont à court terme (des échelles de quelques heures ou mensuelle) alors que la crédibilité de tels modèles est assurée en procédant avec au moins une période d'enregistrement de 30 ans.

1.2 OBJECTIFS

L'objectif de ce présent travail est d'étudier en premier lieu les tendances générales et les ruptures multiples dans le comportement de la vitesse du vent à long terme en Ontario. Ensuite, le second objectif consiste à identifier les indices climatiques de basse fréquence qui influencent la variabilité interannuelle de la vitesse du vent dans la zone d'étude.

1.3 ORIGINALITÉ

Étudier les tendances et les modes de variabilité de la vitesse du vent en Ontario et identifier les indices climatiques d'oscillations de basse fréquence (qui peuvent être utilisés aux fins des prédictions de la vitesse du vent), représente un élément original et qui apporte de nouvelles connaissances sur l'évolution de la puissance éolienne en Ontario, qui est le fer de lance de l'énergie renouvelable au Canada.

1.4 ORGANISATION DE LA SYNTHÈSE

Ce chapitre de synthèse est divisé en cinq parties. La section 1 inclut l'introduction. La section 2 présente la zone d'étude et fournit des renseignements sur les données utilisées. La section 3 présente brièvement les méthodes utilisées. La section 4 fournit un résumé des résultats. La section 5 présente les conclusions et les perspectives.

2 ZONE D'ETUDE ET VARIABLES UTILISEES

L'Ontario couvre une superficie d'environ 1076,395 km^2 . Cette province est située dans le centre-est du pays entre les latitudes 41,5° et 57°N et les longitudes 74,5° et 95,5°W. Elle est bordée par la Baie de James au nord, les Grands Lacs au sud, le Québec à l'est et le Manitoba à l'ouest. L'Ontario est à la pointe de la capacité de production d'énergie éolienne au pays. Par conséquent, il est important d'étudier la variabilité et les tendances à long terme de la vitesse du vent dans cette province. La base de données est constituée de 15 stations horaires de vitesse du vent dispersées dans la zone d'étude et disposant d'au moins 30 ans de données utilisables. Les observations disponibles dans la région nord de l'Ontario sont limitées. Enfin, les variables de vitesse du vent moyenne et maximale annuelles ont été calculées à partir des données horaires selon l'année civile s'étendant du 1er janvier au 31 décembre. La base de données historiques des séries chronologiques de vitesse du vent horaire fournie par Environnement Canada est accessible à l'adresse suivante : <http://climate.weather.gc.ca>.

3 MÉTHODES

Afin d'étudier et d'analyser la variabilité hydro-climatique en Ontario, on commence par une analyse de stationnarité à long terme des variables de vitesse du vent annuelles suivie par une détection des ruptures brusques. Ensuite une analyse de corrélation est complétée dans le but d'explorer et caractériser les liens de dépendance entre les vitesses du vent annuelles et les indices climatiques à grande échelle. Finalement, afin de quantifier le contenu fréquentiel et temporel et de confirmer les résultats de corrélation, on procède une analyse en ondelettes entre la vitesse du vent et les variables climatiques.

Les explications et les formules de base de chacune des méthodologies appliquées sont présentées dans l'article. Dans les sous-sections qui suivent, les différentes approches statistiques utilisées sont résumées brièvement.

3.1 Analyse de tendance à long terme

Suivant la recommandation de l'Organisation météorologique mondiale (Mourato et al. 2010, Nalley et al. 2013), et compte tenu que le test de tendance de Mann-Kendall (MK), présenté par Mann (1945) et Kendall (1967), peut détecter des fausses tendances lorsqu'une autocorrélation positive est détectée, nous avons utilisé une version revisitée du test MK qui applique une correction à la variance de la statistique du test standardisée pour éliminer l'effet d'autocorrélation dans une série. Une fois la correction est appliquée, le test de MK modifié examine la différence de signes entre les points antérieurs et postérieurs. En d'autres termes, si les valeurs de signe ont tendance à augmenter ou à diminuer constamment, alors une tendance positive ou négative se détecte dans la série chronologique donnée. L'hypothèse nulle du test mentionné, H_0 , est que les données sont issues d'une population avec des observations indépendantes et identiquement distribuées. L'hypothèse alternative, H_1 , signifie une présence de tendance dans les données.

Depuis son introduction, le test de MK a été fréquemment utilisé dans le but d'évaluer les tendances temporelles dans les données hydro-climatologiques (Fiala et al. 2010, Khaliq et al. 2008, Ouarda et al. 2021).

3.2 Méthode Bayésienne de détection de multiples points de changement

Un point de changement peut être défini par une rupture brusque à des moments inconnus dans les caractéristiques statistiques des données, telles que la moyenne et la variance ou les coefficients du modèle de régression. La méthode Bayésienne de détection de points de

changement multiples est utilisée dans cette étude afin d'identifier le nombre, la position et l'ampleur des points de changement dans les données (Seidou and Ouarda 2007, Seidou et al. 2007). L'approche repose sur une régression linéaire multiple entre une variable de réponse et des variables explicatives. Si aucune variable explicative n'est spécifiée, le changement est détecté dans le temps.

L'approche Bayésienne de détection de multiples points de changement continue à être une méthode répandue pour analyser les ruptures dans les séries hydro-climatologiques (Ehsanzadeh et al. 2013, Beaulieu et al. 2009, Ouarda et al. 2014).

3.3 Analyse de corrélation

Afin d'identifier les oscillations climatiques qui influencent la variabilité interannuelle des vitesses du vent en Ontario, le calcul du coefficient de corrélation de Pearson a été effectué entre les séries des vitesses maximales et moyennes annuelles et les valeurs précédentes des modèles climatiques moyennées sur trois mois en allant de janvier (Janvier-Février-Mars ; JFM) à octobre (Octobre-Novembre-Décembre ; OND). Le degré de signification statistique est évalué en utilisant le test t de Student. Ensuite, t_r est associée à une valeur p en comparant sa valeur avec la table de la distribution t à $n-2$ degrés de liberté.

3.4 Analyse spectrale en ondelettes

La variabilité temporelle d'une série chronologique peut être analysée par plusieurs méthodes. Par exemple, la transformée de Fourier permet d'étudier la variabilité fréquentielle d'un signal donné mais aucune information n'est fournie sur comment ces modes de variabilité varient à l'échelle temporelle. Dans la présente étude, l'analyse en ondelettes (Torrence and Compo 1998), une technique de traitement de signal, est utilisée afin d'étudier la périodicité des signaux, identifier les non stationnarités et les ruptures dans les données et caractériser le degré de dépendance à l'échelle de cohérence entre deux signaux dans le domaine temps-fréquence. Cette méthode décompose le signal en sous-ondelettes en se basant sur une fonction analysante appelée ondelette-mère. L'ondelette de Morlet est la plus recommandée pour les signaux hydro-climatologiques vu qu'elle représente adéquatement ce type de signaux et fournit un équilibre optimal entre les localisations fréquentielles et temporelles (Jevrejeva, 2003). L'analyse spectrale en ondelettes comporte une analyse d'ondelette continue qui permet d'étudier la périodicité des séries de vitesse du vent, suivie d'une analyse de corrélation croisée afin d'identifier les régions de puissance commune et élevée entre les séries de vitesse du vent et les séries des indices

climatiques. Finalement, une analyse de la cohérence par ondelette dans le but d'identifier les régions où les deux séries co-varient dans l'espace temps-fréquence. Cette analyse spectrale a fait preuve de sa pertinence dans l'analyse des signaux hydrologiques et climatiques non-stationnaires (Chandran et al. 2016; Jevrejeva, 2003, Labat et al., 2002).

4 RÉSULTATS

Dans l'analyse de tendance générale, la détection des ruptures et l'identification des liens de corrélation, la période d'enregistrement a un impact énorme sur l'efficacité des méthodes. Comme la base de données originale contient des séries de données de différentes périodes avec des données manquantes au milieu des séries, nous avons effectué un contrôle de données pour finir avec 15 stations de vitesse du vent avec des données utilisables et des périodes d'enregistrement d'au moins 34 ans de données.

L'analyse de tendance linéaire montre que la plupart des séries de vitesse du vent annuelles présentent des non stationnarités à un degré de confiance statistique de 95%. Les valeurs de la statistique Z_s obtenues pour toutes les séries non-stationnaires sont négatives, ce qui signifie que toutes ces séries présentent des tendances temporelles à la baisse (décroissantes).

Tandis que le test de tendance suggère une tendance à la baisse dans toutes les séries de vitesse du vent significativement non-stationnaires, la procédure Bayésienne de détection de points de changement multiples fournit plus de détails sur l'évolution à long terme de la vitesse du vent. Les résultats confirment les tendances à la baisse observées dans les séries des extrêmes de vent. D'autre part, des tendances croissantes pendant les trois dernières décennies sont révélées par cette approche confirmant le sens de l'évolution de la puissance éolienne en Ontario.

Le but de cette étude est d'identifier les indices climatiques de basse fréquence qui peuvent prédire la vitesse future du vent. L'analyse des liens de corrélation montre que le NAO, PDO et EA sont les indices les plus dominants dans la zone d'étude. L'analyse spectrale en ondelettes a permis de confirmer la consistance des liens de corrélation établis et de caractériser les modes principaux de la variabilité interannuelle de la vitesse du vent dans la zone d'étude. Des corrélations significatives fortes entre l'indice NAO et les vitesses du vent annuelles se produisent principalement pendant les mois d'hiver (JFM). Ces résultats sont conformes aux études antérieures menées dans l'est du Canada et dans d'autres régions de l'hémisphère Nord.

5 CONCLUSIONS ET PERSPECTIVE

La majorité des stations de vitesse du vent présentent des tendances significatives à la baisse. L'approche Bayésienne de détection de points de changement multiples semble confirmer la tendance à la baisse observée dans les stations de vitesse de vent extrême. Inversement, cette méthode a révélé que la plupart des séries de vitesse moyenne présentent des tendances à la hausse au cours des trois dernières décennies. Une analyse de corrélation nous a permis de retenir trois modèles climatiques dominants dans la zone d'étude, l'indice EA, NAO et PDO. Les résultats de l'analyse spectrale en ondelettes ont permis non seulement de confirmer l'influence pertinente de ces trois oscillations climatiques sur les vitesses annuelles du vent (maximales et moyennes) mais aussi d'identifier les non-stationnarités et les variations cycliques différentes (échelles interannuelle, décennale et multi-décennale) de la vitesse du vent en Ontario. Précisément, l'influence est plus prononcée entre les indices retenus et les vitesses annuelles moyennes appuyant la nécessité d'intégrer les indices climatiques dans les modèles de prédition saisonnière de la puissance éolienne.

Dans la perspective de ce travail, les indices EA, NAO et PDO seront utilisés en tant que prédicteurs de la vitesse du vent à long terme en Ontario afin de garantir des modèles de prévision du vent appropriés pendant la durée de vie d'une éolienne (environ 30 ans).

6 RÉFÉRENCES

- Alexiadis, M. C., dokopoulos, P. S., sahsamanoglou, H. S., & manousaridis, I. M. (1998). SHORT term forecasting of wind speed and related electrical power. *Solar energy*, 63(1), 61-68.
- Beaulieu, C., seidou, O., ouarda, T.B.M.J., and X. Zhang (2009). Intercomparison of homogenization techniques for precipitation data continued: Comparison of two recent Bayesian change point models, *Water Resources Research*, 45, W08410, doi: 101029/2008WR007501.
- Chandran, A., Basha, G., and T.B.M.J. Ouarda, (2016). Influence of Climate Oscillations on Temperature and Precipitation over the United Arab Emirates, *International Journal of Climatology*, 36(1): 225-235. DOI:10.1002/joc.4339.
- Ehsanzadeh, E., Saley, HM, Ouarda, T.B.M.J., Burn, D.H., Pietroniro, A., Seidou, O., Charron, C., and D. LEE (2013). Analysis of changes in the Great Lakes hydro-climatic variables, *Journal of Great Lakes Research* 39 (3), 383-394.
- Fiala, T., Ouarda, T. B. M. J., & Hladny, J. (2010). Evolution of low flows in the Czech Republic. 393, 206–218. <https://doi.org/10.1016/j.jhydrol.2010.08.018>
- Hurrell, J.W. and Deser, C. (2010) North Atlantic climate variability: The role of the North Atlantic Oscillation. *Journal of Marine Systems* 79(3-4), 231-244.
- Jerez, S., & Trigo, R. M. (2013). Time-scale and extent at which large-scale circulation modes determine the wind and solar potential in the Iberian Peninsula. *Environmental Research Letters*, 8(4), 044035.
- Jevrejeva, S., Moore, J. and Grinsted, A. (2003) Influence of the Arctic Oscillation and El Niño-Southern Oscillation (ENSO) on ice conditions in the Baltic Sea: The wavelet approach. *Journal of Geophysical Research: Atmospheres* 108(D21).
- Kendall, M.G. and Stuart, A. (1967). The Advanced Theory of Statistics. Population (18^e année), 396-396.
- Khaliq, M.N., Ouarda, T.B.M.J., Gachon, P. and L. Sushama (2008). Temporal evolution of low-flow regimes in Canadian rivers, *Water Resources Research*. 44, W08436.
- Labat, D., Ababou, R. and Mangin, A. (2002) Analyse multirésolution croisée de pluies et débits de sources karstiques. *Comptes Rendus Géoscience* 334(8), 551-556.

- Mann, H.B. (1945) Non-parametric tests against trend. *Econometrica: Journal of the econometric society*, 245-259.
- Mourato, S., Moreira, M., & Corte-Real, J. (2010). Interannual variability of precipitation distribution patterns in Southern Portugal. *International Journal of Climatology*, 30(12), 1784-1794.
- Naizghi, M.S. and Ouarda, T.B.M.J. (2016) Teleconnections and analysis of long-term wind speed variability in the UAE. *International Journal of Climatology* 37(1), 230-248.
- Nalley, D., Adamowski, J., Khalil, B., & Ozga-Zielinski, B. (2013). Trend detection in surface air temperature in Ontario and Quebec, Canada during 1967–2006 using the discrete wavelet transform. *Atmospheric Research*, 132, 375-398.
- Ouarda, T. and Charron, C. (2021) Non-stationary statistical modelling of wind speed: A case study in eastern Canada. *Energy Conversion and Management* 236, 114028.
- Ouarda, T.B.M.J., Charron, C., Niranjan Kumar, K., Marpu, P., Ghedira, H., Molini, A., Khayal, I. (2014). Evolution of rainfall regime in the UAE, *Journal of Hydrology*, 514 (June): 258–270.
- Seidou, O., and T.B.M.J., Ouarda (2007). Recursion-based multiple changepoint detection in multivariate linear regression and application to river streamflows, *Water Resources Research*. 43, W07404, 1-18.
- Seidou, O., Asselin, J.J., and T.B.M.J., Ouarda (2007). Bayesian multivariate linear regression with application to changepoint models in hydrometeorological variables, *Water Resources Research*. 43, W08401, doi:10.1029/2005WR004835, 1-17.
- Thiombiano, A.N., ElAdlouni, S., St-Hilaire, A., Ouarda, T.B.M.J. and El-Jabi, N. (2017). Nonstationary frequency analysis of extreme daily precipitation amounts in Southeastern Canada using a peaks-over-threshold approach, *Theoretical and Applied Climatology*, 129(1-2): 413-426.
- Torrence, C. and Compo, G.P. (1998). A practical guide to wavelet analysis. *Bulletin of the American Meteorological Society* 79(1), 61-78.

CHAPITRE 2: Inter-annual variability and teleconnections of wind speed: case study of Ontario, Canada

Inter-annual variability and teleconnections of wind speed: A case study of Ontario, Canada

Khaoula Laazibi¹, Taha B.M.J. Ouarda¹

1: Canada Research Chair in Statistical Hydro-Climatology, INRS-ETE, Quebec, Canada

This article will be submitted for publication in the Wind energy, Energy for sustainable development, Environmental modeling and assessment.

August 2021

Credit authorship contribution statement:

K. Laazibi: Conceptualization, Methodology, Software, Formal analysis, Investigation, Data curation, Visualization, Writing – original draft.

T.B.M.J. Ouarda: Conceptualization, Methodology, Validation, Investigation, Supervision, Writing – review & editing, Funding acquisition.

ABSTRACT: Predictions based on very short wind speed records have compromised wind energy assessment as they disregard inter-annual variability and existing long-term trends. The main objectives of the study are to study the inter-annual variability of wind speeds in Ontario (east-central Canada) and examine their links with relevant large-scale atmospheric circulation patterns. Long record wind speed series at 15 meteorological stations in Ontario are used to assess long-term trends and detect possible change points in maximum and mean annual wind speeds. The modified Mann-Kendall test results indicate that several stations present significant wind speed trends at the 5% level. However, all the significant trends were decreasing on the annual timescale. The Bayesian change-point detection method unveiled rising trends during the last three decades in a large number of mean wind speed time-series. About twice as many stations displayed abrupt changes during the 1985-1995 and 2005-2015 periods, while the majority (80%) occurred during 1965-1975. Linear correlation and cross-correlation analysis revealed the potential impact of the East Atlantic (EA), North Atlantic Oscillation (NAO), and the Pacific Decadal Oscillation (PDO) climate indices on long-term wind speed variability in the study region. As we approach the Atlantic Ocean, the impact of the first two patterns is much more pronounced.

KEY WORDS Wind speed; variability; teleconnection; trend; change point; wavelet analysis; climate index; Ontario.

1. Introduction

The Canadian wind energy industry has mainly developed in three provinces: Ontario, Quebec, and Alberta. The province of Ontario holds the title of Canada's leader for wind power, with 5,436 megawatts (MW) of installed electricity generating capacity as of December 2019. Since 2014, Ontario has implemented a low-carbon economy by replacing its electricity generation sources contributing to global warming, such as coal and oil, with new renewable and sustainable power sources like wind energy. The province is also using its new green-energy law to help promote economic growth.

Wind speed and wind power share a cubic relationship. Consequently, a relatively slight increase in wind speed estimates results in a significant increase in power production and, hence, on the economics of wind energy projects. Assessing the wind energy potential based on very short wind records, such as a few years, ignores the information regarding the inter-annual variability and the decadal trends in wind characteristics. Occasionally, these assessment efforts fail to deliver the expected results once the project is complete (Woldesellasse et al. 2020). For this reason, higher awareness of such information is essential for industry insurance.

Due to data homogeneity issues, there have been far fewer trend analyses on wind speed data than temperatures or precipitation time-series (Brázdil et al. 2009, Pryor and Barthelmie 2003, Tuller 2004). For mid-latitude sites (e.g., in China (Zhang et al. 2019) and the United States (Pryor et al. 2009)), historical near-surface wind speed data sets revealed significant decreasing trends over the past 30-50 years. Pryor et al. (2009) found that most observational time-series over the United States for the period 1973-2005 showed a decrease in wind speeds at the 50th and 90th percentiles. Similarly, using homogenized near-surface wind speed data sets, Wan et al. (2010) found

significant decreasing (increasing) trends throughout western Canada and most parts of southern Canada (central Canadian Arctic) in all seasons. Wang et al. (2006) confirmed that the observed short-term trends in Canada's wind speed depended on latitude. Several explanations and causes are proposed in the literature for the decreasing trends detected in low-surface wind speed observations (Hurrell and Deser 2010, Wang et al. 2006).

The literature recognizes the prominent effects of multiple large-scale atmospheric circulation patterns on climate variability in the tropical Atlantic (Thiombiano et al. 2018). According to Hurrell and Deser (2010), variations in atmospheric circulation patterns significantly influence wind speed variability. In terms of climatology, these relationships are referred to as "teleconnections" (Alexander et al. 2002, Ouachani et al. 2013). Much of the published studies pay particular attention to multiscale climate patterns influencing hydrological components, such as streamflow and precipitation, on both regional and global scales (Lee and Ouarda 2010, Ouarda et al. 2014, Regonda et al. 2005, Tremblay et al. 2011). Wang et al. (2006) revealed that Canadian cyclone activity was significantly related to the NAO, the PDO, and the El Niño–Southern Oscillation (ENSO) indices. The NAO was best suited to explain cyclone variance and the most prominent mode of variability in the North Atlantic. According to Abhishek et al. (2010), the Pacific North American (PNA) teleconnection pattern showed the most significant association with long-term trends in hourly wind speed over three cities in the Midwest U.S.. The Arctic Oscillation (AO) and the Nino-3.4 sea surface temperature (SST) anomalies were both related to monthly wind speeds in Minnesota, in the upper Midwest U.S. (Klink 2007).

Recently, Naizghi and Ouarda (2016) used historical wind speed time-series and reanalysis data sets to identify the dominant teleconnection patterns over the United Arab Emirates. They

indicated that the region's wind speed was mainly associated to the NAO and the EA during the summer, and to the ENSO and the Indian Ocean Dipole (IOD) indices during winter and autumn. More recently, Sinha et al. (2020) addressed the relationship between Indian Ocean wind speeds and ENSO climate indices. They reported varying correlations between the ENSO indices in different areas of the Indian Ocean. Ouarda and Charron (2021) indicated that, over the eastern Canadian region, the NAO is the most significant circulation index during the winter and the PNA is the most significant during the spring season. Based on the preliminary studies of Lee et al. (2021) the monthly ENSO and PDO teleconnection patterns showed the most significant links to the net basin supply (NBS) of the Great Lakes system.

Since there have been very few studies assessing long-term wind speed over the province of Ontario, the extent of wind speed variability and factors influencing it remain barely known. This study covers 15 stations located in Ontario with hourly wind speed data to identify atmospheric circulation teleconnections with the most significant influence on wind speeds in the study region, which can be used as covariates in future long-term wind speed prediction studies.

2. Data sets description

A total of two primary sources provided the data used in this study. First, hourly wind speed data were derived from fifteen meteorological stations located all over Ontario. The second dataset contains the selected climate patterns hypothesized to influence wind speed variability in the study area.

2.1 Region of study and wind speed data

The province of Ontario is located in central-eastern Canada, covering an area of approximately $1076,95 \text{ km}^2$. As illustrated in Figure 1 (a), Quebec borders Ontario to the east and northeast,

James Bay to the north, the Great Lakes and the U.S. states to the south, and Manitoba to the west. The province is at the leading edge of Canada's wind power capacity by taking up 36% of the country's current capacity of wind-generated electricity. The Canadian Wind Energy Association indicates that Ontario's capacity will continue to rise significantly in the coming years (Yao et al. 2012). It is hence important to analyze long-term patterns of wind speed variability in the province to provide reliable estimates of future wind capacity. The database consisted of 15 hourly wind speed stations located throughout the province with at least 30 years of useable data. Several stations have a recording period of 68 years. Figure 1 illustrates the locations of the 15 stations and indicates that there is limited information in Ontario's northern region. The seasonal and annual mean and maximum wind speed variables were computed using hourly data according to the calendar year spanning January 1st to December 31st. The historical database of hourly wind speed time-series provided by Environment Canada can be accessed at: <http://climate.weather.gc.ca>. A brief description of each wind speed station is provided in Table 1.

2.2 Climate pattern data

Climate oscillations are characterized by cyclical fluctuations recurring at various timescales within the global or regional climate. The major long-scale climate indices were considered based on the literature to assess their impact on the annual (maximum and mean) wind speed in Ontario. The main monthly climate indices associated with climate variability in North America were obtained from the NOAA Physical Sciences Laboratory database, available at <https://psl.noaa.gov/data/climateindices/list/>. The following climate indices were included in this study: The NAO, the NAOJ (Jones et al. 1997), the AO, the PDO, the PNA, the EA, the Tropical Northern Atlantic (TNA), the Atlantic Multi-decadal Oscillation (AMO), and the Western

Hemisphere Warm Pool (WHWP). Additionally, various indices driven from SST and SLP anomalies over different Pacific regions were used to measure the strength of ENSO teleconnections, namely the Nino3.4 and the Southern Oscillation Index (SOI). The name, short name, and record period of each climate index used in this study are given in Table 2.

3. Description of applied research methods

An overview of each of the methods used in the present study is provided in the following subsections. Statistical hypothesis trend testing, Bayesian multiple change-point detection, linear correlation analysis and wavelet analysis are four of the methods used in this study.

3.1 Mann-Kendall trend test

Following the recommendation provided by the World Meteorological Organization (WMO), we used the Mann-Kendall trend test (Kendall and Stuart 1967, Mann 1945) to detect linear and non-linear long-term trends at each selected wind speed station. As the chosen test is non-parametric, no assumptions were made regarding the normality of the data. This approach examines the difference in signs between earlier and later points. In other words, if the sign values tend to increase or decrease constantly, then there is a positive or negative trend in the time-series.

The null hypothesis for the MK test, H_0 , is that data are independent and identically distributed (iid) over time. Hence, H_0 indicates no monotonic trend in the data series, while the alternative hypothesis, H_1 , points to a significant trend. From a statistical perspective, rejecting the null hypothesis means that the data cannot be considered iid. Nevertheless, from a practical perspective, the non-acceptance of H_0 implies the presence of a trend over time (H_1).

Test computation begins with an estimation of its statistic, referred to as S , and calculated as follows:

$$S = \sum_{i=1}^{ss-1} \sum_{j=i+1}^{ss} sgn(x_j - x_i) \quad \text{where} \quad sgn(x_j - x_i) = \begin{cases} +1 & \text{if } x_j - x_i > 0 \\ 0 & \text{if } x_j - x_i = 0 \\ -1 & \text{if } x_j - x_i < 0 \end{cases} \quad (1)$$

where x_j and x_i are time-series observations in chronological order, $j>i$, and ss represents the sample size.

For samples larger than 8, the S statistic's distribution approaches the Gaussian form (normal distribution) with zero mean ($E(S) = 0$) and variance σ_s^2 calculated as follows:

$$\sigma_s^2 = \frac{[ss(ss-1)(2ss+5) - \sum_{j=1}^p t_j(t_j-1)(2t_j+5)]}{18} \quad (2)$$

where p is the number of tied values and t_j is the number of ties for the j^{th} value.

As a second step, the standardized test statistic Z_s is calculated as follows:

$$Z_s = \begin{cases} \frac{S-1}{\sigma_s} & \text{if } S > 0 \\ 0 & \text{if } S = 0 \\ \frac{S+1}{\sigma_s} & \text{if } S < 0 \end{cases} \quad (3)$$

Finally, based on the normal cumulative distribution tables, the p-values for the MK test are as follows:

$$p = 2 \times \left[1 - \left(\frac{1}{\sqrt{2\pi}} e^{-\frac{1}{2}|Z_s|^2} \right) \right] \quad (4)$$

At the significance level of α , a trend is considered statistically significant if $|Z_s|$ is greater than $Z_{I-(\alpha/2)}$.

A positive (negative) value of Z_s indicates a significant upward (downward) trend.

The presence of serial correlation in a series increases the possibility of detecting false trends, which is why several versions of the MK test were proposed in the literature to incorporate the lag-1 autocorrelation in the series. The modified MK test selected for this study computes the autocorrelation coefficient in the first place. Before computing the MK trend test, lag-1 autocorrelation, if significant at a level α , is corrected with the variance correction, and serial correlation is removed (Hamed and Rao 1998). This study presents results for the modified MK test at significance levels of 5% and 10% to examine long-term trends in wind speed over Ontario.

3.2 Change Point Detection Analysis

The Bayesian multiple change-point detection procedure of Seidou and Ouarda (2007) is employed in this study to detect chronological changes in the behavior of annual wind speed time-series. This approach is intended to identify the number, position, and magnitude of change points in the relationship between the variable of interest and a set of independent variables. Seidou et al. (2006) developed a change-point model that allows inferring only one change point when applied to a multivariate regression equation. Through a segmentation technique, Seidou and Ouarda (2007) generalised their change-point model to the case of multiple change points in a given series.

In a dataset consisting of n observations and m explanatory variables, the response variable is denoted by y_j ($j=1,\dots,n$), while the j^{th} observation of the i^{th} explanatory variable is denoted by x_{ij} ($i=1,\dots,m; j=1,\dots,n$). Thus, in multiple linear regression, the following can be written:

$$y_j = \sum_{i=1}^m \theta_i x_{ij} + \varepsilon_j, \quad (j = 1, \dots, n) \quad (5)$$

As part of this case study, we intend to detect chronological changes in the annual wind speed time-series (i.e., no explanatory variables are specified). In Seidou and Ouarda (2007), the mathematical formulation behind this procedure and the inferences regarding the number and position of change points are described in full detail.

3.3 Correlation Analysis

Linear correlation analysis using Pearson's correlation coefficient (PCC) at a 5% significance level is adopted in this research to understand the inter-relation between annual wind speeds and the low-frequency climate oscillations hypothesized to be potential covariates in the study area. Because the available data sets differ in their records, a matching period of data is first needed to be defined for both variables and covariates. Then, the PCC between the annual maximum and annual mean wind speeds and the climate oscillation indices time-series using a moving average window of three months from January (January-February-March; JFM) to October (October-November-December; OND) at each station. As a final step, the moving average of three-month period is used as a smoother for the climate oscillation series to ensure greater accuracy in the correlation links and the wavelet analysis performed afterwards.

The correlation coefficient, r , is derived by calculating covariance between two continuous variables; X and Y , based on the following formula:

$$r = \frac{n \sum XY - (\sum X)(\sum Y)}{\sqrt{n \sum X^2 - (\sum X)^2} \sqrt{n \sum Y^2 - (\sum Y)^2}} \quad (6)$$

where n indicates the sample size for each variable.

The PCC's statistical significance is assessed by testing the null hypothesis, H_0 , which states that there is no coherence between the two variables ($r=0$), against the alternative hypothesis, H_1 , which assumes that a correlation exists between the two data sets ($r \neq 0$). The test statistic, referred to as t_r , is defined as:

$$t_r = r \sqrt{\frac{n - 2}{1 - r^2}} \quad (7)$$

Once t_r is calculated, a p -value is obtained by comparing t_r 's value with the t-table distribution with the $n-2$ degrees of freedom.

3.4 Wavelet analysis

Wavelet analysis proved its relevance in identifying signals affected by non-stationarity (Grinsted et al. 2004, Torrence and Compo 1998), but also in the study of co-variability between several hydrological variables and climate indices in frequency and time domains (Thiombiano et al. 2017, Chandran et al. 2015, Jevrejeva et al. 2003, Labat et al. 2002).

Continuous Wavelet Transform (CWT), cross-wavelet transform (XWT), and wavelet coherence (WTC) are employed in this research. In addition to statistically studying the relationships between dominant large-scale climate oscillations and wind speeds in the study region, we sought more stable signal decomposition. The CWT, XWT and WTC plots capture the changes in timescale in and between the climate oscillations and wind speed time-series.

According to Torrence and Compo (1998), the CWT is a complete representation of a signal in both the time and scale domains through varying the translation and the scale parameter of the mother wavelet function $\Psi_0(\eta)$ continuously. Therefore, obtaining adequate results requires a

crucial choice of the mother wavelet function since the frequency and time resolution are proportional to the width of the mother wavelet used. In this case study, the Morlet wavelet function remains the best candidate. Jevrejeva et al. (2003) reported that the Morlet is frequently considered for most hydro-climatological variables since it adequately represents the signal's shape and allows an optimum balance between time and frequency localization (Labat 2005, Naizghi and Ouarda 2016). Furthermore, the selected mother wavelet is widely applied to the analysis of tidal signals since it meets the wavelet admissibility condition (i.e., the wavelet must oscillate with a mean equal to zero) (Farge 1992, Guo et al. 2015).

The XWT enables identifying regions of high common power in the time-frequency space between two time-series X and Y based on their CWTs; $Wn\ X(s)$, and $Wn\ Y(s)$, respectively. Time-series showing powerful common features suggests potential teleconnection between the two signals. Nevertheless, since the XWT is not a normalized measure, one must keep in mind that it shows signs of significant high powers not only if the X and Y co-vary but also when a significant-high power is observed in one of the time-series (Naizghi and Ouarda 2016).

As a compromise to the XWT's shortcomings, the WTC is applied in this research to test the statistical significance of relationships between climate patterns and wind speed (Maraun and Kurths 2004). The WTC measures the intensity of the correlation between two series in the time-frequency domain (Jevrejeva et al. 2003) regardless of whether they have strong common power. Henceforth, the XWT and WTC approaches provide valuable and complementary information.

As a way to assess the statistical significance at a level of 5%, we applied the significance test elaborated by Torrence and Compo (1998), employing a Monte Carlo simulation through a red

noise process based on the autocorrelation functions of the two data series as detailed by Grinsted et al. (2004).

In mathematics, The CWT, denoted by W_n is the convolution of a continuous signal x_n with the local basis function $\Psi_{n,s}(\eta)$, a translated and compressed or expanded version of $\Psi_0(\eta)$, and reads as:

$$W_n^X(s) = \int_{-\infty}^{+\infty} x(t) \Psi_{n,s}^* dt \quad \text{where} \quad \Psi_{n,s} = \frac{1}{\sqrt{s}} \Psi_0 \left(\frac{t-n}{s} \right) \quad (8)$$

where s designates the scale parameter, n the translation parameter, and the asterisk * designates the complex conjugate of the wavelet.

The Morlet function is written in the following form:

$$\Psi_0(\eta) = \pi^{-\frac{1}{4}} e^{i \omega_0 \eta} e^{-\frac{1}{2} \eta^2} \quad \text{where} \quad \eta = st \quad (9)$$

where ω_0 denotes a dimensionless frequency while η denotes a dimensionless time (Grinsted et al. 2004).

According to Torrence and Compo (1998), the XWT denoted W , is created by multiplying the complex wavelet transform of X and the complex conjugate of Y as:

$$W_n^{XY}(s) = W_n^X(s) W_n^{Y*}(s) \quad (10)$$

Based on Torrence & Webster (1999), the WTC of two series is given as follows:

$$R_n^2 = \frac{|S(s^{-1} W_n^{XY}(s))|^2}{S(s^{-1} |W_n^X(s)|^2) \cdot S(s^{-1} |W_n^Y(s)|^2)} \quad (11)$$

A general introduction to Morlet wavelets, as well as a general overview of its application to geophysical and oceanographic studies, are provided in Torrence and Compo (1998). The source code for the wavelet software package used in this article is available at: <https://pol.ac.uk/home/research/waveletcoherence/>.

4. Results and discussion

4.1 Long-term trend analysis results

The Mann-Kendall test and its modified version are applied to 15 wind speed time-series to detect seasonal and annual trends. Since the modified MK trend test is more reliable in the presence of serial correlation, only the results of the modified version are given and discussed. Table 3 provides Z_s values obtained at each station for each wind speed variable where statistical significance is evaluated at the 0.05 and 0.1 levels. The superscripts *a* and *b* to the Z_s statistics indicate that the trend is statistically significant at the 5 and 10% levels, respectively.

The Z_s values obtained for annual variables indicate that major wind speed time-series show statistically significant decreasing trends at the 5% level. As detailed in Table 3, significant trends at the 10% level are observed in 13 (86.6%) and 9 (60%) of the 15 annual maximum and mean wind speed time-series, respectively. However, several detected trends are significant at the 5% level. In terms of maximum, Wiarton station (14) indicates the most pronounced downward trend ($Z_s=-5.55$), while for the annual average, Trenton (13) shows the most downward trend ($Z_s=-3.96$).

The seasonal timescales are also studied by splitting the year into four seasons as shown in Table 3. Similar to the annual timescale, most stations exhibit significant negative trends, which is the case of the four seasons. Furthermore, the Z_s statistics obtained for all seasons reveal that no significant increasing trends were detected in any station. For the average, the number of stations showing significant negative trends in mean wind speed data is higher during summer and autumn. Eleven (73.3%) of the 15 stations show decreasing trends in summer and autumn at the 10% level. While for the maximum, the number of stations showing significant negative trends is higher during winter and spring. Significant decreasing trends in maximum wind speed data were detected at 11 (73.3%) and 10 (66.7%) of the 15 stations in the winter and spring.

Moreover, the annual and seasonal wind speed trend analysis reveals that increasing trends are detected only in two stations (Toronto L. B. P. (12) and Geraldton (1)), and none of these increasing trends are significant. For Thunder Bay (9), the mean and the maximum annual wind speed have significant decreasing trends at the 10% level. On a seasonal time scale, this same station shows downward trends during all seasons, and several trends are significant at the 5% level.

Many authors have highlighted the statistically significant decreasing trends occurring in observational wind speed data over North America (Pryor et al. 2009; Wan et al. 2010). Our evidence presented thus far supports the obtained decreasing trends in the seasonal and annual wind speed series. Previous studies originally referred to the decline of near-surface wind speeds as "global stilling" (Blunden et al. 2018, Roderick et al. 2007). In a recent paper, Zhang et al. (2019) found that the increased surface friction was predominant in the long-term decline of surface wind speeds in the northern hemisphere during 1973-2014. Nevertheless, it is equally

important to mention that atmospheric circulation and turbulent friction contribute significantly to this reduction.

4.2 Bayesian procedure results

The results of this approach are detailed in tabular form. Table 4 gives a summary of the Bayesian change-point detection results for both annual maximum and annual mean wind speed data. Considering the necessity to stay away from the edges of the series to avoid edge effects (Ouarda et al. 2014), the minimum segmentation (threshold) values considered in this study are 5 years of data. This threshold represents the minimal length of a stationary segment. We checked the results for segments with at least 3 and 4 years of data, and they were consistent with those with 5 and 6 years, yet with more change points detected frequently near the edges.

The Bayesian approach was first applied to yearly maximum wind speed data. Results carried out with segments of 5 years differ slightly from those with 6-years. Seven (46.7%) of 15 maximum wind speed time-series showed a single shift. No significant change was detected at 6 (40%) maximum wind speed series. Annual mean wind speed data were then analysed. Table 4 shows that multiple shifts at all stations but Toronto Buttonville (11), where only one change was detected around 1994. This station has the shortest record period (34 years).

Note that the year in which the change occurred may be one or two years earlier or later than the detected date (Ouarda et al. 2014). Considering this, about twice as many stations exhibit abrupt changes during the 1985-1995 and 2005-2015 periods, and most detected changes (80%) in the mean wind speed data that occurred around 1965-1975. From a global perspective, 2010 was a year marked by a mean warm anomaly on a global scale, especially in Canada, Greenland, North Africa, and the Middle East (Cattiaux et al. 2010). While the negative phase of NAO dominated

in winter 2010, the cold record of winter 1963 seemed to be caused by both the negative NAO and strong Scandinavian blockings (Cattiaux et al. 2010). The extreme persistence of the negative phase of the NAO index may be a contributing factor to the detected shifts occurring during the 2005-2015 and 1965-1975 periods. Several studies reported changes in the North Atlantic atmospheric circulation patterns between the late 1960s and early 1970s that appear to coincide with 80% of the observed shifts in mean wind speed between 1965 and 1975 (Hodson et al. 2014). Large portions of Canada and other regions experienced abnormally cold and snowy weather conditions during the 1995/1996 winter season (DJF) (Halpert et al. 1996). Halpert and Bell (1997) reported that the reason behind this was mean temperatures averaging below normal. Additionally, during this winter season, periods of extreme cold and snow alternated with short periods of warmth and rain marking the variability considerably over large regions of the United States and Canada. A phenomenon of this kind has not occurred since 1985. These factors may explain the multiple changes occurring during the period 1985-1995 in annual wind speed data.

Figure 2 (a) depicts the results of the Bayesian multiple change-point procedure at Thunder Bay station, indicating two opposite trends in the maxima time-series. Indeed, the general trends observed in maximum wind speed data were positive until 1998, marking the start of a new decreasing epoch. The results displayed in Figure 2 (b) show a unique behavior in the maxima time-series at the Wiarton station (14). A marked decreasing trend was detected, confirming the modified MK test results where the most extreme negative trend was recorded at this station ($Z_s = -5.55$). For the annual average time-series, the significant changes in wind speeds at the Thunder Bay station (9) seem to occur around the 1960s (1963, 1969) and the 1980s (1982, 1987). Unlike the modified MK test results, change detection reveals that a slight increase in trend is observed from the end of the 1980s to the end of the recording period (Figure 2 (c)). A similar pattern, but

one with fewer shifts, can be seen in Figure 2 (d), where a significant increasing trend is observed from 1990 to 2019 at Wiarton station (14). In contrast to MK test results that indicate decreasing trends in both variables, the multiple change-point detection procedure reveals a positive trend in several mean wind speed time-series over the past three decades.

4.3 Correlation Analysis results

One of the purposes of this study is to identify the dominant climate indices that can predict future wind speed on an annual time scale. To this end, linear correlation analysis was performed between yearly wind speed variables (maxima time-series and means time-series) and monthly climate indices time-series taken over a three-month moving average window. The computation of Pearson's correlation coefficient at a significance level of 5% shows a significant correlation was found between all the annual mean and maxima of hourly wind speed time-series and at least one of the climate indices as detailed in Table 5.

As reported by Table 5, NAO, PDO and EA are the most important climate oscillation patterns in the study area since they exhibit strong correlations with the largest percentage of maximum and mean wind speed time-series over Ontario. Other selected climate indices show statistically significant correlation coefficients; however, these values are too low to provide a meaningful explanation for the inter-annual variability of wind speed.

The correlation coefficient between annual wind speeds and the NAO index ranges between ± 0.28 and 0.53 on average and ± 0.28 and 0.59 on maximum. Figures 3 (a) and (b) shows that there is an east-west gradient between annual wind speeds and the NAO. In other words, the NAO impacts are more pronounced as we get closer to the Atlantic, while they are less noticeable as we get closer to the Pacific. Also, all stations exhibit an opposite relationship with the NAO, except two

stations, Sault Sainte Marie (6) considering the annual maxima time-series and Geraldton (1) considering the annual mean time-series. Figures 3 (c) and (d) show the relationship between annual wind speed amounts and the PDO index. Given that we are dealing with the decadal oscillations in the Pacific, we expected to observe greater significance and intensity in the western side of the province, which is not the case. This may be related to Ontario's relative proximity to the Atlantic and Arctic Oceans, compared to the Pacific Ocean. All stations show negative correlations with the PDO, except Geraldton (1) (Geraldton (1) and Toronto Buttonville (11)), which shows a similar behavior when considering the maximum and mean time-series. Note that these two stations have the shortest record periods. The PDO seems to have more significant effects on extreme wind speeds over the western region. In contrast, stronger associations between mean wind speed amounts and the PDO index are registered over the eastern region with PCCs ranging from ± 0.26 to 0.56. A high correlation exists between wind speeds over Ontario and the EA index (Figures 3 (e) and (f)). Similarly to NAO, the impacts of the EA are stronger as we get closer to the Atlantic. An opposite behavior is observed when studying the maximum and mean time-series for all stations except for Sault Sainte Marie (6) and Toronto L. B. P. (12), respectively. Interestingly, stations located close to the same geographic longitude, 80°W , exhibit the strongest correlations with the EA oscillations.

Only significant negative correlations are observed between the three dominant climate oscillation patterns and wind speed at Thunder Bay station. A negative correlation exists between annual maximum (mean) wind speed and the NAO index between the months of January-April (January-May), as shown in Table 6. Likewise, the NAO index exhibits the same pattern at the Wiarton station during the same time period (Table 7). Another important finding is that both stations recorded their highest negative correlation coefficient during January-February-March (JFM).

Results confirm those of Ouarda and Charron (2021) who identified the NAO as a major circulation mode in eastern Canada during the winter season (JFM). Additionally, the PDO shows negative correlations with the annual mean wind speed at Thunder Bay station during the January-May period. The highest correlation coefficients occurred during March-April-May (MAM), which is also the case for extreme wind speed data. On the other hand, the Wiarton station shows a significant negative correlation between the PDO and annual maximum (mean) wind speed data during the January-April (January-August) period. The more surprising correlation is with the EA index, which exhibits a negative relationship with annual wind speed over the study region. On average, significant negative PCCs observed at Wiarton station range from 0.25 to 0.47. At the same time, extreme wind speeds show significant correlation coefficients throughout the entire period, with relatively higher values ranging from 0.33 to 0.48.

4.4 Wavelet analysis results

4.4.1 Cross-correlation analysis results

Figure 4 illustrates the XWT plots between mean wind speeds at Thunder Bay and Wiarton stations and the three most important climate indices. Observations at Thunder Bay station reveal significant shared features between mean wind speed and the prominent mode of high-scale variability, the EA, over the months OND in the 7–10 year-band during the two decades (1960–980) (Figure 4(a)). The arrows in this significant pattern indicate the opposite phase difference between the two signals, agreeing with the significant negative correlation shown by the linear correlation analysis. This finding is in agreement with the findings of Zubiate et al. (2017) showing strong negative correlations between wind speeds and the EA index in the mid-North Atlantic region.

The NAO index and mean annual wind speed reveal significant power between the 5–7 and 7–10 year bands, respectively, from 1962 to 1972 and 1972 to 1984 during the months of JFM (Figure 4(c)). The strongest and longest duration signal observed between the PDO index and annual wind speed in the 9–11 year period during the months of MAM lasts two decades (1960–1980) where the two signals show an anti-phase behavior. On the other hand, the strongest and longest signal observed between the PDO index and annual wind speed in the 9–11 year period during the months of MAM lasts two decades (1960–1980), and the two signals show an anti-phase behavior. Again, in line with the correlation analysis results, the XWT results confirm the strong negative association between the PDO and wind speeds. Nevertheless, the cross-wavelet analysis conducted between the three dominant climate indices and annual wind speeds at Thunder Bay station reveals no significant patterns since the early 1980s. After the early 1980s, the annual mean wind speed time-series had low wavelet power (no significant features were observed after 1984), explaining the unexpected result. Also, related to this might be the winter NAO experiencing an inter-decadal transition in intensity and position around the 1980s (Hurrell 1995, Jung and Hilmer 2001, Jung et al. 2003). Compared to the Thunder Bay station, the relationship between wind speeds at Wiarton and the three climate indices shown by the XWT plots is weak. The majority of patterns appear in the range of 2–4 years, except for the XWT of NAO and wind speed, where a tiny pattern stands out as a slight common feature in the ~5–7 year band.

Overall, the XWT plots at Thunder Bay and Wiarton stations between extreme wind speeds and the three dominant climate indices follow an almost identical pattern to the one recorded in mean wind speeds at Wiarton, but with a slight increase in the signal strength. It seems that most of the activity is observed around the 2–3 years band, except for the common feature observed in the 5–7 years band between NAO and maximum wind speeds at Thunder Bay station during the JFM

period (Figure 5 (c)). Comparing mean findings with those of extreme values confirms that teleconnections are much more potent between mean wind speeds and teleconnection patterns.

Even though the results obtained at the Wiarton station are not in agreement with the correlation analysis results, it does confirm that WTC is a complementary tool to the cross-correlation analysis, and accordingly required in this research. In fact, if two time-series have low wavelet power but still have a high coherence value, then wavelet coherence is the better approach.

4.4.2 Wavelet coherence analysis results

Figures 6 and 7 display the WTC plots between mean and extreme wind speed data, respectively, at the Thunder Bay and Wiarton stations and the EA, NAO and PDO indices. Figure 6 (a) illustrates the WTC between the EA and the annual mean wind speed over Thunder Bay station during the months of OND. The plot indicates that the EA index shows strong coherence with annual wind speeds at Thunder Bay in the time period of 7–10 years from 1953 to 2010, where the two signals are in an opposite phase difference. The anti-phase relationship indicates that a positive phase of the climate index results in lower wind speed. Also, the EA reveals significant coherence in the 17–24 year band between 1953–1986, starting with an in-phase behavior and ending with wind speed leading the EA index. Similar behavior is observed in the 2–4 year band from 2000 till 2013.

At Wiarton, the EA exhibits strong positive coherence with annual wind speed on a larger scale; the 14–22 year band during the months of OND from 1955 to 2019 as displayed in Figure 6 (b). In addition to the 2–4-year period where strong interactions between the EA and mean wind speed are found from 2005 to 2018.

The WTC of NAO and mean wind speed at Thunder Bay station during the months of January to March is illustrated in Figure 6 (c). Strong coherence zones are observed in the range of 5–7 years,

beginning first from 1953 to the middle of the 1970s, where the NAO is leading wind speed, followed by an in-phase behavior from 1980 till 2000. Furthermore, NAO reveals strong coherence with an anti-phase difference in the 14-16 year period from 1953 to 1975. Similar behavior is observed at Wiarton station during the same period (JFM), with additional small but strong coherence zones appearing at higher frequencies (Figure 6(d)). Unsurprisingly, the large-scale mode PDO exhibits high and persistent coherence in the lower frequency domain during the months of March-May as observed by the most prominent pattern in the 16-24 year band at both stations (Figure 6 (e) and (f)). A second strong but short-lasting pattern is observed from the middle 1980s till 2000 in the 3–6 year band where wind speed at Thunder Bay station is leading the large-scale decadal pattern.

Less long-lasting patterns are observed between the extreme wind speeds and the three climate indices (Figure 7). A decadal pattern is observed between the EA index and maximum wind speed at the Thunder Bay station from 1953 to 1980 followed by less long-lasting coherence zones appearing at higher frequencies (Figure 7(a)). Regarding extreme annual wind speeds at the Wiarton station, the most important climate index is the EA during the months of JJA. Figure 7 (b) depicts the entire activity organized in the 2-10 year period between extreme wind speeds and the EA pattern demonstrating a strong negative relationship, which is in line with correlation analysis findings. The NAO index seems to be the most associated with extreme wind speeds at the Thunder Bay station (Figure 7 (c)). The PDO during the MAM period shows no significant features associated with the extreme wind speeds at the Thunder Bay station since 1970. However, a tiny significant pattern appears in the 2-3 year band starting from 2010 and lasting over half decade (Figure 7(e)).

5. Conclusions and future work

Beginning with a long-term trend analysis using 15 wind speed time-series located in Ontario, this study allows us to conclude that the majority of stations here exhibit significant decreasing trends in maximum velocity. Nevertheless, a few stations showed increasing trends on the annual and seasonal timescales, but none of these stations were significant at the 10% level. These findings are consistent with previous studies (Pryor et al. 2009). The Bayesian multiple change-point detection approach appeared to support the decreasing trend observed in extreme wind speed stations. Conversely, this method revealed that most mean wind speed series exhibit increasing trends over the last three decades. Results with segments of 5 and 6 years were remarkably similar for both of the annual variables.

Correlation analysis and wavelet analysis (both WTC and XWT) were carried out for the preceding three-monthly moving average values of the various climate patterns and annual wind speed data. This investigation enabled us to retain three dominant climate patterns in the study area: EA, NAO, PDO indices. The XWT plots revealed that the link between annual wind speed data and the retained climate indices is much more important when considering the mean wind speed time-series. Additionally, these potent teleconnections are in an opposite phase difference with the maximum and mean wind speed data. Strong significant correlations between the NAO index and wind speeds in Ontario mostly occur during the winter (JFM) months. Results are in line with earlier studies conducted in eastern Canada and other Northern Hemisphere regions. Then again, the EA and PDO mostly influence annual wind speeds during the autumn (OND) and spring (MAM) months. Taking everything into account, the findings of this study provided some of the most significant factors affecting wind speeds over Ontario.

In wind energy prediction models, teleconnection patterns are among the most reliable covariates for their predictable nature and prominent influence on wind speed. As a perspective to this work, the EA, NAO, and PDO patterns can be used as predictors for long-term forecasting of wind speed in Ontario to guarantee proper wind prediction models during the lifetime of wind farms (about 30 years).

References

- Abhishek, A., Lee, J.Y., Keener, T.C. and Yang, Y.J. (2010) Long-term wind speed variations for three midwestern U.S. cities. *J Air Waste Manag Assoc* 60(9), 1057-1064.
- Anctil, F. and Coulibaly, P. (2004) Wavelet analysis of the interannual variability in southern Québec streamflow. *Journal of Climate* 17(1), 163-173.
- Blunden, J., Hartfield, G., Arndt, D., Dunn, R., Tye, M., Blenkinsop, S., Donat, M., Durre, I., Ziese, M. and Cooper, O. (2018) State of the Climate in 2017. *Bulletin of the American Meteorological Society* 99(8), Si-S310.
- Brázdil, R., Chromá, K., Dobrovolný, P. and Tolasz, R. (2009) Climate fluctuations in the Czech Republic during the period 1961-2005. *International Journal of Climatology* 29(2), 223-242.
- Cattiaux, J., Vautard, R., Cassou, C., Yiou, P., Masson-Delmotte, V. and Codron, F. (2010) Winter 2010 in Europe: A cold extreme in a warming climate. *Geophysical Research Letters* 37(20).
- Chandran, A., Basha, G. and Ouarda, T.B.M.J. (2015) Influence of climate oscillations on temperature and precipitation over the United Arab Emirates. *International Journal of Climatology* 36(1), 225-235.
- Farge, M. (1992) Wavelet transforms and their applications to turbulence. *Annual review of fluid mechanics* 24(1), 395-458.

Grinsted, A., Moore, J.C. and Jevrejeva, S. (2004) Application of the cross wavelet transform and wavelet coherence to geophysical time-series. *Nonlinear processes in geophysics* 11(5/6), 561-566.

Guo, L., van der Wegen, M., Jay, D.A., Matte, P., Wang, Z.B., Roelvink, D. and He, Q. (2015) River-tide dynamics: Exploration of nonstationary and nonlinear tidal behavior in the Yangtze River estuary. *Journal of Geophysical Research: Oceans* 120(5), 3499-3521.

Halpert, M. S., G D. Bell, V. E. Kousky, and C. F. Ropelewski, 1996: Climate assessment for 1995. *Bull Amer. Meteor. Soc.*, 77(5), S1-S44.

Halpert, M.S. and Bell, G.D. (1997) Climate assessment for 1996. *Bulletin of the American Meteorological Society* 78(5s), S1-S50. Hamed, K.H., Rao, A.R., 1998. A modified Mann–Kendall trend test for autocorrelated data. *J. Hydrol.* 204 (1–4), 182–196.

Hodson, D. L. R., Robson, J. I., & Sutton, R. T. (2014). An Anatomy of the Cooling of the North Atlantic Ocean in the 1960s and 1970s, *Journal of Climate*, 27(21), 8229-8243. Retrieved Nov 2, 2021.

Hurrell, J.W. (1995) Decadal trends in the North Atlantic Oscillation: Regional temperatures and precipitation. *Science* 269(5224), 676-679.

Hurrell, J.W. and Deser, C. (2010) North Atlantic climate variability: The role of the North Atlantic Oscillation. *Journal of Marine Systems* 79(3-4), 231-244.

Jevrejeva, S., Moore, J. and Grinsted, A. (2003) Influence of the Arctic Oscillation and El Niño–Southern Oscillation (ENSO) on ice conditions in the Baltic Sea: The wavelet approach. *Journal of Geophysical Research: Atmospheres* 108(D21).

Jones, P.D., Jónsson, T. and Wheeler, D. (1997) Extension to the North Atlantic Oscillation using early instrumental pressure observations from Gibraltar and south-west Iceland. *International Journal of Climatology: A Journal of the Royal Meteorological Society* 17(13), 1433-1450.

Jung, T. and Hilmer, M. (2001) The link between the North Atlantic Oscillation and Arctic sea ice export through Fram Strait. *Journal of Climate* 14(19), 3932-3943.

Jung, T., Hilmer, M., Ruprecht, E., Kleppek, S., Gulev, S.K. and Zolina, O. (2003) Characteristics of the recent eastward shift of interannual NAO variability. *Journal of Climate* 16(20), 3371-3382.

Kendall, M.G. and Stuart, A. (1967) The Advanced Theory of Statistics. *Population (18^e année)*, 396-396.

Klink, K. (2007) Atmospheric Circulation Effects on Wind Speed Variability at Turbine Height. *Journal of Applied Meteorology and Climatology* 46(4), 445-456.

Labat, D. (2005) Recent advances in wavelet analyses: Part 1. A review of concepts. *Journal of Hydrology* 314(1-4), 275-288.

Labat, D., Ababou, R. and Mangin, A. (2002) Analyse multirésolution croisée de pluies et débits de sources karstiques. *Comptes Rendus Géoscience* 334(8), 551-556.

Lee, T. and Ouarda, T.B. (2010) Long-term prediction of precipitation and hydrologic extremes with nonstationary oscillation processes. *Journal of Geophysical Research: Atmospheres* 115(D13).

Lee, T., Ouarda, T.B. and Seidou, O. (2021) Characterizing and Forecasting Climate Indices Using Time-series Models.

Mann, H.B. (1945) Nonparametric tests against trend. *Econometrica: Journal of the econometric society*, 245-259.

Maraun, D. and Kurths, J. (2004) Cross wavelet analysis: significance testing and pitfalls. *Nonlinear processes in geophysics* 11(4), 505-514.

Michael A., A., Ileana, B. and Matthew, N. (2002) The Atmospheric Bridge: The Influence of ENSO Teleconnections on Air–Sea

Interaction over the Global Oceans. *Journal of Climate* 15, 2205-2231.

Naizghi, M.S. and Ouarda, T.B.M.J. (2016) Teleconnections and analysis of long-term wind speed variability in the UAE. International Journal of Climatology 37(1), 230-248.

Ouachani, R., Bargaoui, Z. and Ouarda, T. (2013) Power of teleconnection patterns on precipitation and streamflow variability of upper Medjerda Basin. International Journal of Climatology 33(1), 58-76.

Ouarda, T. and Charron, C. (2021) Non-stationary statistical modelling of wind speed: A case study in eastern Canada. Energy Conversion and Management 236, 114028.

Ouarda, T.B.M.J., Charron, C., Niranjan Kumar, K., Marpu, P.R., Ghedira, H., Molini, A. and Khayal, I. (2014) Evolution of the rainfall regime in the United Arab Emirates. Journal of Hydrology 514, 258-270.

Pryor, S.C. and Barthelmie, R.J. (2003) Long-term trends in near-surface flow over the Baltic. International Journal of Climatology 23(3), 271-289.

Pryor, S.C., Barthelmie, R.J., Young, D.T., Takle, E.S., Arritt, R.W., Flory, D., Gutowski, W.J., Nunes, A. and Roads, J. (2009) Wind speed trends over the contiguous United States. Journal of Geophysical Research 114(D14).

Regonda, S.K., Balaji, R., Martyn, C. and John, P. (2005) Seasonal Cycle Shifts in Hydroclimatology over the Western United States. Journal of Climate 18, 372-384.

Roderick, M.L., Rotstayn, L.D., Farquhar, G.D. and Hobbins, M.T. (2007) On the attribution of changing pan evaporation. Geophysical Research Letters 34(17).

Seidou, O., Asselin, J.J. and Ouarda, T.B.M.J. (2006) Bayesian multivariate linear regression with application to change point models in hydrometeorological variables. Water Resources Research 43(8).

Seidou, O. and Ouarda, T.B. (2007) Recursion-based multiple changepoint detection in multiple linear regression and application to river streamflows. Water Resources Research 43(7).

- Sinha, M., Jha, S. and Chakraborty, P. (2020) Indian Ocean wind speed variability and global teleconnection patterns. *Oceanologia* 62(2), 126-138.
- Thiombiano, A. N., El Adlouni, S., St-Hilaire, A., Ouarda, T. B., & El-Jabi, N. (2017). Nonstationary frequency analysis of extreme daily precipitation amounts in Southeastern Canada using a peaks-over-threshold approach. *Theoretical and Applied Climatology*, 129(1), 413-426.
- Thiombiano, A. N., St-Hilaire, A., El Adlouni, S. E., & Ouarda, T. B. (2018). Nonlinear response of precipitation to climate indices using a non-stationary Poisson-generalized Pareto model: case study of southeastern Canada. *International Journal of Climatology*, 38, e875-e888.
- Torrence, C. and Compo, G.P. (1998) A practical guide to wavelet analysis. *Bulletin of the American Meteorological Society* 79(1), 61-78.
- Tremblay, L., Larocque, M., Anctil, F. and Rivard, C. (2011) Teleconnections and interannual variability in Canadian groundwater levels. *Journal of Hydrology* 410(3-4), 178-188.
- Tuller, S.E. (2004) Measured wind speed trends on the west coast of Canada. *International Journal of Climatology* 24(11), 1359-1374.
- Wan, H., Swail, V.R. and Wang, X.L. (2010) Homogenization and Trend Analysis of Canadian Near-Surface Wind Speeds. *Journal of Climate* 23(5), 1209-1225.
- Woldesellasse, H., Marpu, P.R. And Ouarda, T.B.M.J. (2020). Long-term forecasting of wind speed in the UAE using nonlinear canonical correlation analysis (NLCCA), *Arabian Journal of Geosciences*, 13(18): 962. doi:10.1007/s12517-020-05981-9.
- Wang, X.L., H.Wan and Swail, V.R. (2006) Observed Changes in Cyclone Activity in Canada and Their Relationships to Major Circulation Regimes. *Journal of Climate* 19, 896-915.
- Yao, Y., Huang, G. H., & Lin, Q. (2012). Climate change impacts on Ontario wind power resource. *Environmental Systems Research*, 1(1), 1-11.
- Zhang, R., Zhang, S., Luo, J., Han, Y. and Zhang, J. (2019) Analysis of near-surface wind speed change in China during 1958–2015. *Theoretical and Applied Climatology* 137(3-4), 2785-2801.

Zubiate, L., McDermott, F., Sweeney, C. and O'Malley, M. (2017) Spatial variability in winter NAO–wind speed relationships in western Europe linked to concomitant states of the East Atlantic and Scandinavian patterns. *Quarterly Journal of the Royal Meteorological Society* 143(702), 552–562.

LIST OF TABLES

TABLE 1: GEOGRAPHICAL COORDINATES AND TIME-SERIES LENGTHS OF THE 15 WIND SPEED STATIONS.....	49
TABLE 2: CLIMATE OSCILLATION PATTERNS USED IN THIS STUDY.	50
TABLE 3: Z-VALUES OF THE MODIFIED MANN-KENDALL TEST FOR THE PRESENCE OF TREND IN MAXIMUM AND MEAN ANNUAL AND SEASONAL WIND SPEED TIME-SERIES FOR THE 15 STATIONS IN ORDER OF TABLE 1 (^ TREND IS STATISTICALLY SIGNIFICANT AT P-VALUE < 0.05; ^B TREND IS STATISTICALLY SIGNIFICANT AT P-VALUE < 0.1).	51
TABLE 4 : SUMMARY OF BAYESIAN CHANGE-POINT DETECTION ANALYSIS WITH SEGMENT OF 6 YEARS.	52
TABLE 5: PERCENTAGE OF STATIONS SHOWING SIGNIFICANT CORRELATIONS WITH CLIMATE INDICES	53
TABLE 6: LINEAR CORRELATION COEFFICIENTS BETWEEN ANNUAL WIND SPEED AT THUNDER BAY STATION (9) AND THE THREE CLIMATE PATTERNS: EA, NAO, AND PDO.....	54
TABLE 7: LINEAR CORRELATION COEFFICIENTS BETWEEN ANNUAL WIND SPEED AT WIARTON STATION (14) AND THE THREE CLIMATE PATTERNS: EA, NAO, AND PDO.	55

Table 1: Geographical coordinates and time-series lengths of the 15 wind speed stations.

#	Station name	Latitude (°N)	Longitude (°W)	Elevation (m)	Length (years)
1	Geraldton	49.8	-86.9	339.6	39
2	Kapuskasing	49.4	-82.5	226.5	68
3	Kenora	49.8	-94.4	409.7	68
4	London	43.0	-81.2	278.0	68
5	Ottawa	45.3	-75.7	79.2	68
6	Sault Sainte Marie	46.5	-84.5	192.0	59
7	Sioux Lookout	50.1	-91.9	383.1	68
8	Sudbury	46.6	-80.8	348.4	67
9	Thunder Bay	48.4	-89.3	199.0	68
10	Timmins	48.6	-81.4	335.3	65
11	Toronto Buttonville	43.9	-79.4	198.1	34
12	Toronto L. B. P.	43.7	-79.6	173.4	68
13	Trenton	44.1	-77.5	86.3	68
14	Wiarton	44.7	-81.1	222.2	68
15	Windsor	42.3	-82.9	189.6	68

Table 2: Climate Oscillation Patterns used in this study.

No.	Name	Short name	Period of record
1	Arctic Oscillation	AO	1952-2019
2	Atlantic Multidecadal Oscillation	AMO	1952-2019
3	East Atlantic	EA	1952-2019
4	NINA3.4	Nina3.4	1952-2019
5	North Atlantic Oscillation	NAO	1952-2019
6	North Atlantic Oscillation Jones version	NAOJ	1952-2019
7	Pacific Decadal Oscillation	PDO	1952-2019
8	Pacific North American	PNA	1952-2019
9	Southern Oscillation Index	SOI	1952-2019
10	Tropical Northern Atlantic	TNA	1952-2019
11	Western Hemisphere Warm Pool	WHWP	1952-2019

Table 3: Z-values of the modified Mann-Kendall test for the presence of trend in maximum and mean annual and seasonal wind speed time-series for the 15 stations in order of Table 1 (^a Trend is statistically significant at p-value < 0.05; ^b Trend is statistically significant at p-value < 0.1).

#	Annual		Autumn		Winter		Spring		Summer	
	(Jan-Dec)	Mean	(Oct-Dec)	Mean	(Jan-Mar)	Mean	(Apr-Jun)	Mean	(Jul-Sept)	Mean
1	-1.01	0.42	0.47	0.94	0.00	0.28	-1.65 ^b	-0.02	-1.26	0.72
2	-2.13 ^a	-1.93 ^b	-1.07	-2.63 ^a	-0.74	-1.58	-1.57	-2.04 ^a	-1.43	-2.16 ^a
3	-4.05 ^a	-3.09 ^a	-4.91 ^a	-3.09 ^a	-4.44 ^a	-2.55 ^a	-3.44 ^a	-3.04 ^a	-3.19 ^a	-3.39 ^a
4	-3.28 ^a	-2.91 ^a	-0.91	-2.91 ^a	-3.97 ^a	-4.68 ^a	-3.08 ^a	-3.10 ^a	-2.24 ^a	-2.46 ^a
5	-3.74 ^a	-0.71	-0.18	-0.68	-2.08 ^a	-0.93	-2.13 ^a	-0.94	-1.34	-0.67
6	-4.28 ^a	-1.68 ^b	-2.99 ^a	-1.72 ^b	-2.65 ^a	-2.25 ^a	-2.31 ^a	-2.12 ^a	-1.78 ^b	-2.40 ^a
7	-5.38 ^a	-1.17	-3.41 ^a	-1.43	-1.79 ^b	-0.89	-2.64 ^a	-1.56	-4.01 ^a	-1.81 ^b
8	-4.62 ^a	-2.01 ^a	-5.23 ^a	-3.26 ^a	-4.31 ^a	-2.74 ^a	-4.18 ^a	-2.59 ^a	-6.17 ^a	-2.43 ^a
9	-1.80 ^b	-1.84 ^b	-3.85 ^a	-2.10 ^a	-3.23 ^a	-1.89 ^b	-1.91 ^b	-1.59	-3.50 ^a	-2.79 ^a
10	-3.30 ^a	-1.52	-2.69 ^a	-2.10 ^a	-2.74 ^a	-1.72 ^b	-2.73 ^a	-1.90 ^b	-3.93 ^a	-2.04 ^a
11	-3.13 ^a	-2.17 ^a	-2.48 ^a	-3.55 ^a	-2.88 ^a	-1.38	-1.23	-0.24	-1.52	-2.49 ^a
12	-0.34	0.73	-0.53	0.48	-0.74	0.69	-0.24	1.21	0.06	0.81
13	-3.11 ^a	-3.96 ^a	-1.05	-3.76 ^a	-1.52	-4.42 ^a	-1.33	-4.24 ^a	-1.65 ^b	-3.76 ^a
14	-5.55 ^a	-2.15 ^a	-3.66 ^a	-3.38 ^a	-5.25 ^a	-2.73 ^a	-3.52 ^a	-3.94 ^a	-4.30 ^a	-2.40 ^a
15	-2.56 ^a	-1.088	-1.32	-1.89 ^b	-2.21 ^a	-2.33 ^a	-1.59	-1.15	-1.14	-0.86

Table 4 : Summary of Bayesian change-point detection analysis with segment of 6 years.

#	Annual maximum wind speed				Annual mean wind speed			
	change between 1965-1975	change between 1985-1995	change between 2005-2015	elsewhere	change between 1965-1975	change between 1985-1995	change between 2005-2015	elsewhere
1	-	-	-	-	-	1996	2010	-
2	-	-	-	-	-	1983	2014	1963
3	-	-	-	-	1967; 1974	-	-	-
4	-	-	-	-	1966	-	2005	-
5	-	-	2005; 2014	-	1970	-	2003	1960
6	-	-	-	-	-	1993	2003; 2012	-
7	-	-	-	2002	1969	-	2009	-
8	-	-	2007		-	-	2010	1962
9	1969		-	1998	1969	1987	-	1962; 1982
10	-	1989	-	-	1974	-	2010	1963; 1982
11	-	1994	-	-	-	1994	-	-
12	-	-	-	1960	1973	-	-	1999
13	-	-	-	-	1970	-	-	1961; 1979
14	-	-	-	1960	1972	1991	-	1964
15	1966	-	-	-	-	1995	-	1963

Table 5: Percentage of stations showing significant correlations with climate indices

	Maximum wind speed	Mean wind speed
SOI	46.7	26.7
NINO3	66.7	13.3
AO	46.7	40.0
NAO	73.3	73.3
NAOJ	60.0	73.3
PDO	73.3	73.3
PNA	13.3	66.7
AMO	60.0	46.7
WHWP	46.7	26.7
TNA	53.3	53.3
EA	73.3	80.0

Table 6: Linear Correlation Coefficients between annual wind speed at Thunder Bay station (9) and the three climate patterns: EA, NAO, and PDO.

	JFM	FMA	MAM	AMJ	MJJ	JJA	JAS	ASO	SON	OND	NDJ*	DJF*
Annual maximum wind speed												
NAO	-0.356	-0.299	-0.201	-0.052	0.026	-0.067	-0.116	-0.156	-0.113	-0.062	-0.174	-0.266
PDO	-0.222	-0.240	-0.267	-0.200	-0.188	-0.179	-0.223	-0.248	-0.246	-0.230	-0.211	-0.215
EA	-0.162	-0.131	-0.066	-0.069	-0.116	-0.172	-0.150	-0.214	-0.325	-0.410	-0.384	-0.338
Annual mean wind speed												
NAO	-0.354	-0.315	-0.288	-0.034	0.047	0.070	-0.017	-0.033	-0.110	-0.078	-0.262	-0.286
PDO	-0.273	-0.279	-0.325	-0.282	-0.261	-0.219	-0.200	-0.206	-0.189	-0.169	-0.160	-0.167
EA	-0.347	-0.347	-0.236	-0.154	-0.144	-0.254	-0.227	-0.209	-0.263	-0.391	-0.429	-0.347

Significant correlations at the 5% level are highlighted in bold text.

The asterisk * refers to periods not to be included in this analysis.

Table 7: Linear Correlation Coefficients between annual wind speed at Wiarton station (14) and the three climate patterns: EA, NAO, and PDO.

	JFM	FMA	MAM	AMJ	MJJ	JJA	JAS	ASO	SON	OND	NDJ*	DJF*
Annual maximum hourly wind speed												
NAO	-0.399	-0.415	-0.146	-0.008	0.115	-0.087	0.012	0.185	0.253	0.033	-0.346	-0.412
PDO	-0.389	-0.375	-0.343	-0.286	-0.211	-0.170	-0.116	-0.087	-0.069	-0.091	-0.126	-0.200
EA	-0.361	-0.423	-0.441	-0.361	-0.376	-0.479	-0.424	-0.406	-0.391	-0.414	-0.356	-0.325
Annual mean wind speed												
NAO	-0.587	-0.512	-0.313	0.042	0.141	-0.019	-0.026	0.076	0.094	-0.150	-0.475	-0.502
PDO	-0.288	-0.323	-0.375	-0.322	-0.315	-0.300	-0.304	-0.266	-0.232	-0.232	-0.255	-0.290
EA	-0.302	-0.241	-0.242	-0.202	-0.217	-0.341	-0.327	-0.342	-0.341	-0.470	-0.456	-0.377

Significant correlations at the 5% level are highlighted in bold text.

The asterisk * refers to periods not to be included in this analysis.

LIST OF FIGURES

FIGURE 1 : GEOGRAPHICAL LOCATION OF THE 15 OBSERVATION SITES. STATIONS TARGETED FOR CASE ILLUSTRATION ARE HIGHLIGHTED IN RED.....	57
FIGURE 2: CHANGE-POINT DETECTION FOR ANNUAL MAXIMUM (A; B) AND MEAN (C; D) WIND SPEED DATA RECORDED AT THUNDER BAY (9) AND WIARTON (14) STATIONS.....	58
FIGURE 3: PEARSON'S CORRELATION COEFFICIENT RANGE VALUES ARE SHOWN IN (A) AND (B) FOR NAO, (C) AND (D) FOR PDO AND (E) AND (F) FOR EA AND THE ANNUAL MAXIMUM AND MEAN WIND SPEED VARIABLES RESPECTIVELY, WHERE UPWARD (DOWNWARD) POINTING TRIANGLES INDICATE POSITIVE (NEGATIVE) SIGNIFICANT CORRELATION AT A 5% LEVEL OF SIGNIFICANCE.	59
FIGURE 4: CROSS-CORRELATION ANALYSIS BETWEEN ANNUAL MEAN WIND SPEED DATA AND THE DOMINANT PATTERNS OVER THE THUNDER BAY (9) AND WIARTON (14) STATIONS FOR THE PERIOD 1953-2019. THE VECTORS INDICATE THE RELATIVE PHASE RELATIONSHIP BETWEEN WIND SPEED AND THE CLIMATE INDICES (POINTING RIGHT (LEFT) INDICATES IN-PHASE (ANTI-PHASE) BEHAVIOR; POINTING DOWN (UP) INDICATE THAT THE FIRST (SECOND) SERIES IS LEADING). THE SHARP REGION INDICATES THE CONE OF INFLUENCE (COI). THICK BLACK CONTOURS REPRESENT THE 5% SIGNIFICANCE LEVEL AGAINST RED NOISE PROCESS.....	60
FIGURE 5: SAME AS FIGURE 4 FOR ANNUAL MAXIMUM WIND SPEED DATA.	62
FIGURE 6 : WAVELET COHERENCE BETWEEN ANNUAL MEAN WIND SPEED DATA AND THE DOMINANT PATTERNS OVER THUNDER BAY (9) AND WIARTON (14) STATIONS FOR THE PERIOD 1953-2019. THE STRENGTH OF THE COHERENCE IS DISPLAYED BY THE COLOR BAR.	63
FIGURE 7: SAME AS FIGURE 6 FOR ANNUAL MAXIMUM WIND SPEED DATA.	64

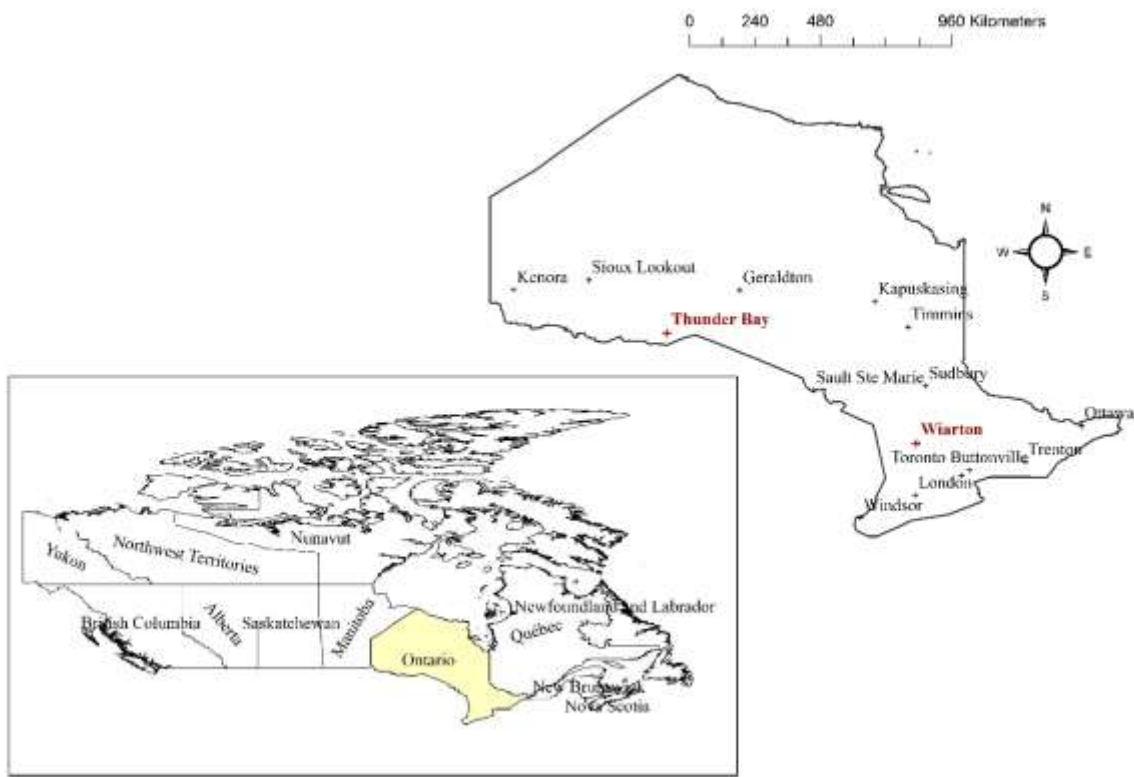


Figure 1 : Geographical location of the 15 observation sites. Stations targeted for case illustration are highlighted in red.

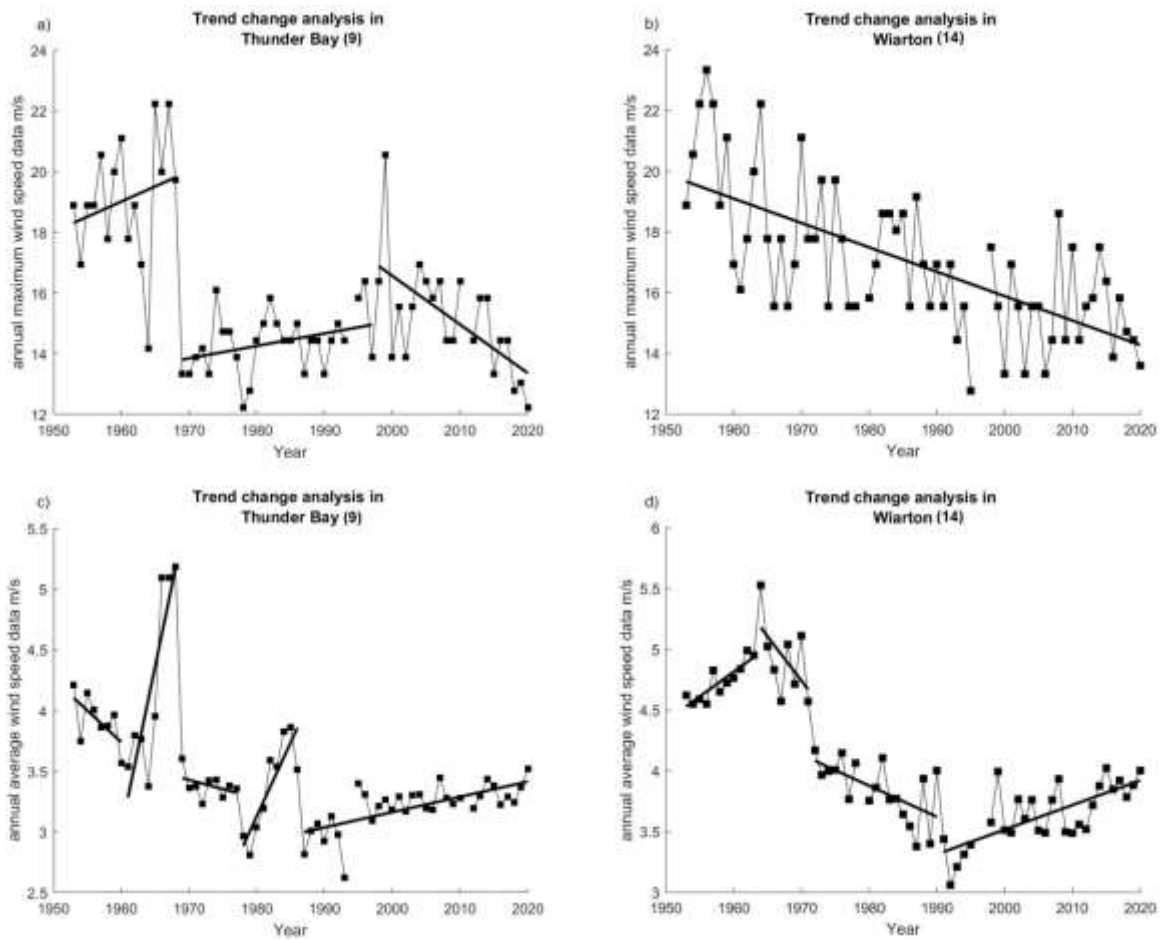


Figure 2: Change-point detection for annual maximum (a; b) and mean (c; d) wind speed data recorded at Thunder Bay (9) and Wiarton (14) stations.

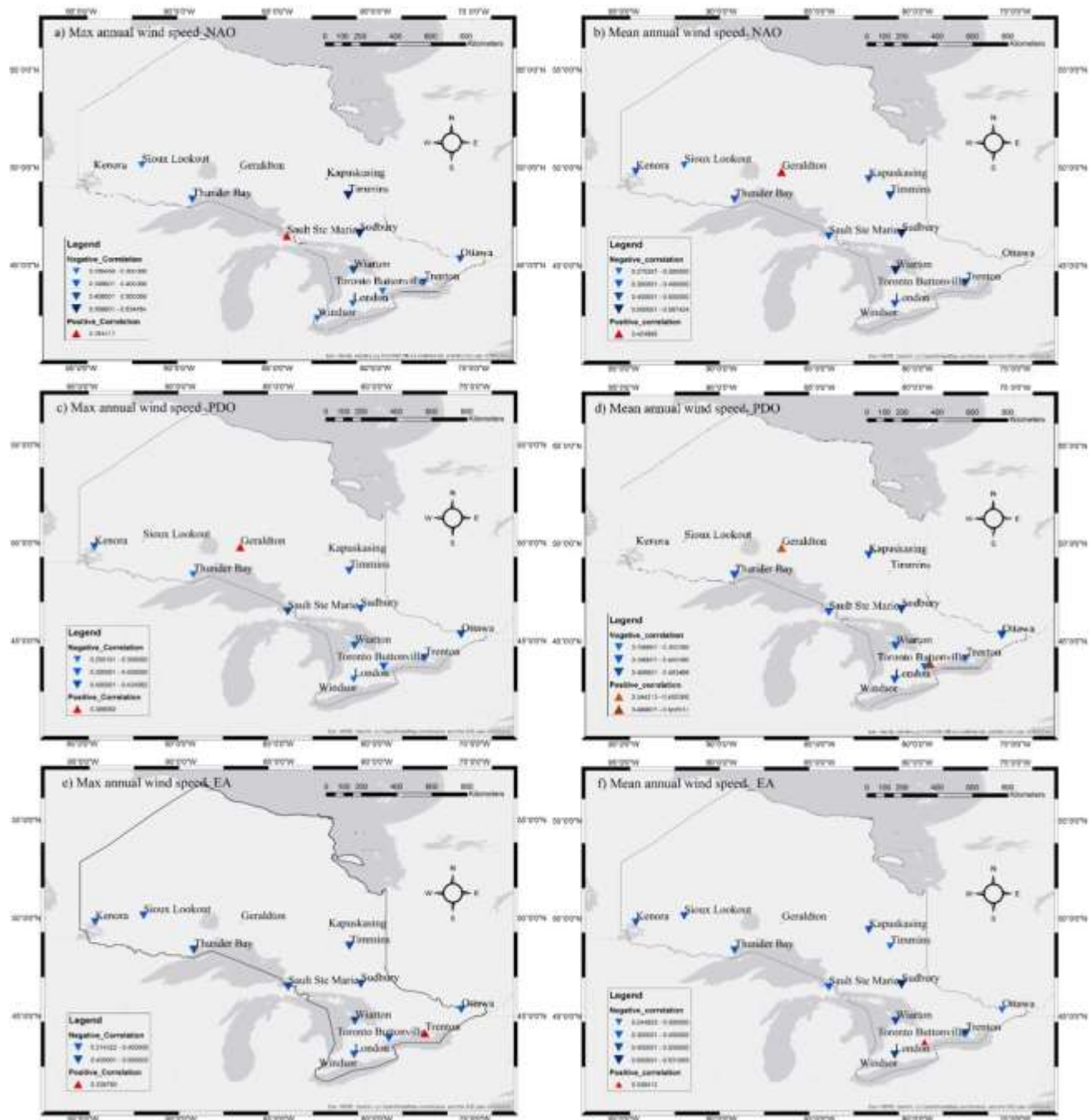


Figure 3: Pearson's correlation coefficient range values are shown in (a) and (b) for NAO, (c) and (d) for PDO and (e) and (f) for EA and the annual maximum and mean wind speed variables respectively, where upward (downward) pointing triangles indicate positive (negative) significant correlation at a 5% level of significance.

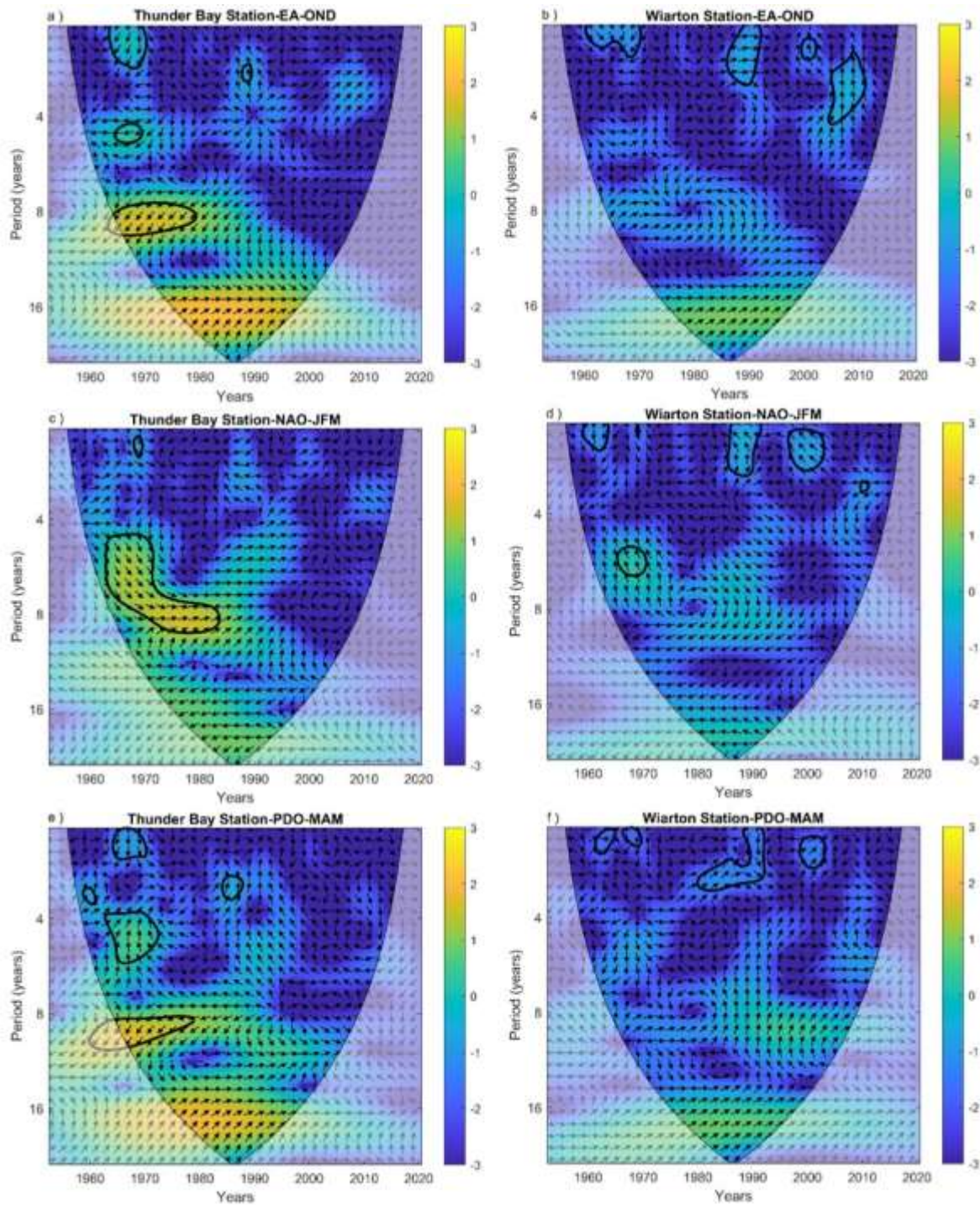


Figure 4: Cross-correlation analysis between annual mean wind speed data and the dominant patterns over the Thunder Bay (9) and Wiarton (14) stations for the period 1953-2019. The vectors indicate the relative phase relationship between wind speed and the climate indices (pointing right)

(left) indicates in-phase (anti-phase) behavior; pointing down (up) indicate that the first (second) series is leading). The sharp region indicates the Cone of Influence (COI). Thick black contours represent the 5% significance level against red noise process.

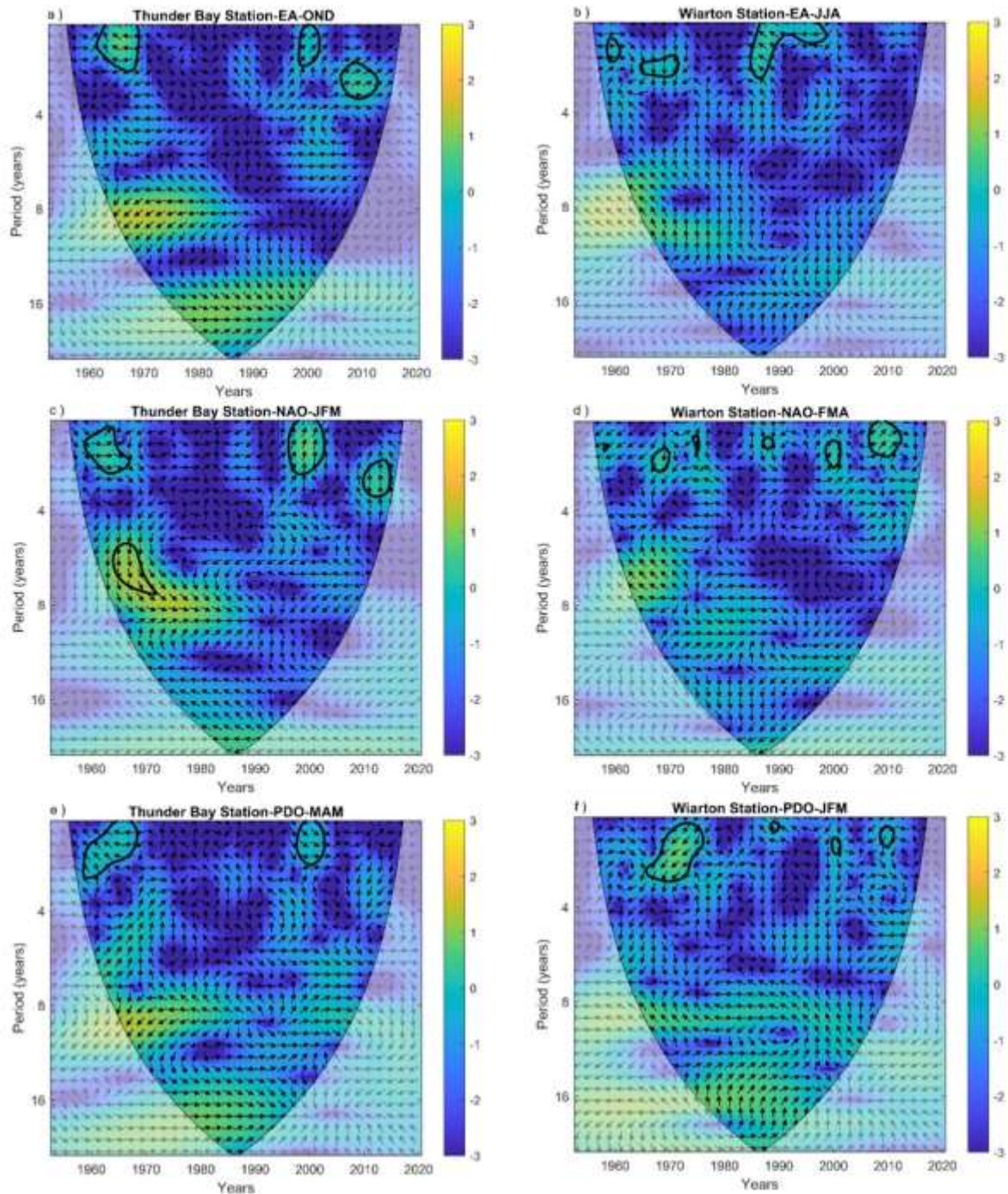


Figure 5: Same as Figure 4 for annual maximum wind speed data.

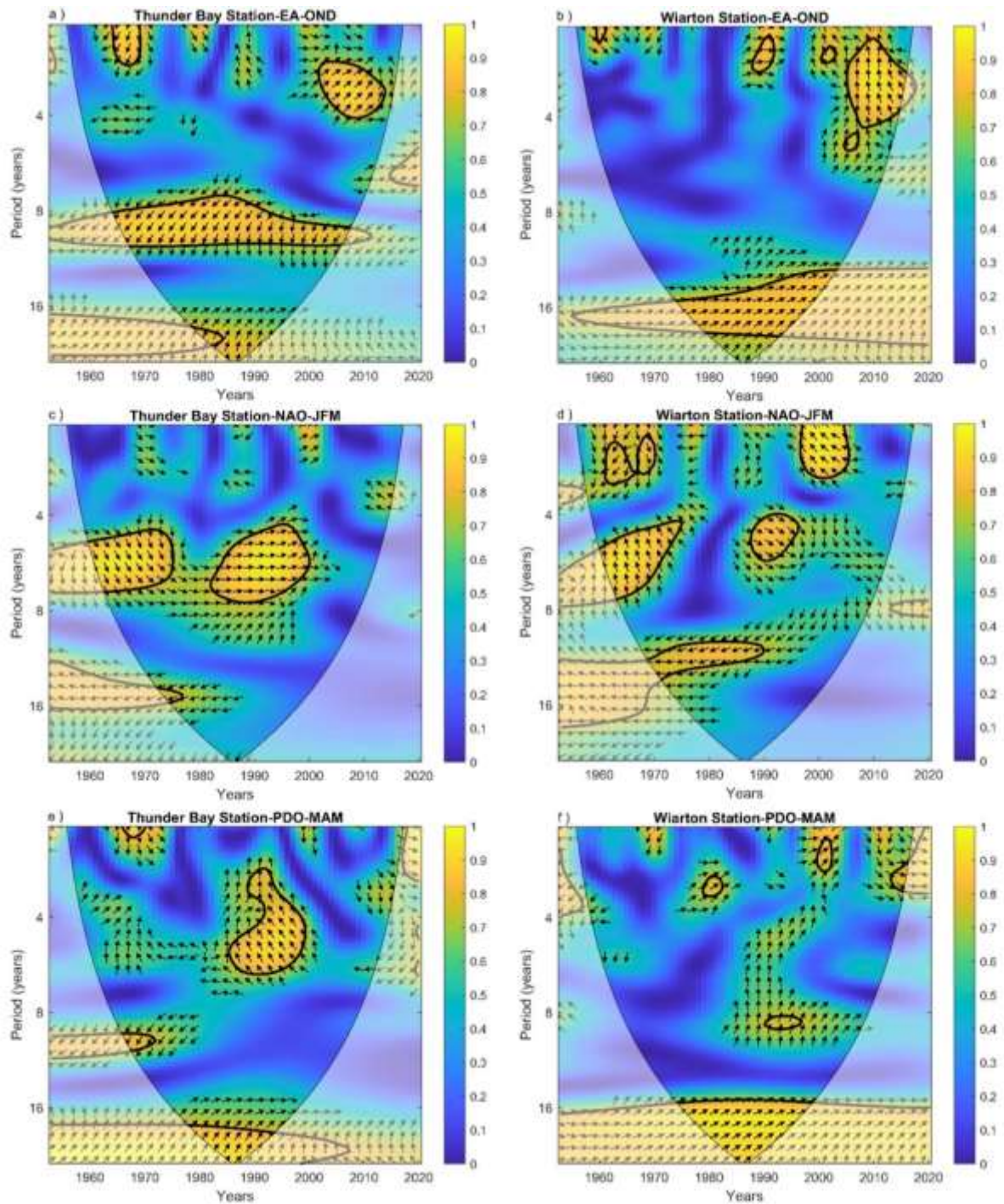


Figure 6 : Wavelet coherence between annual mean wind speed data and the dominant patterns over Thunder Bay (9) and Wiarton (14) stations for the period 1953-2019. The strength of the coherence is displayed by the color bar.

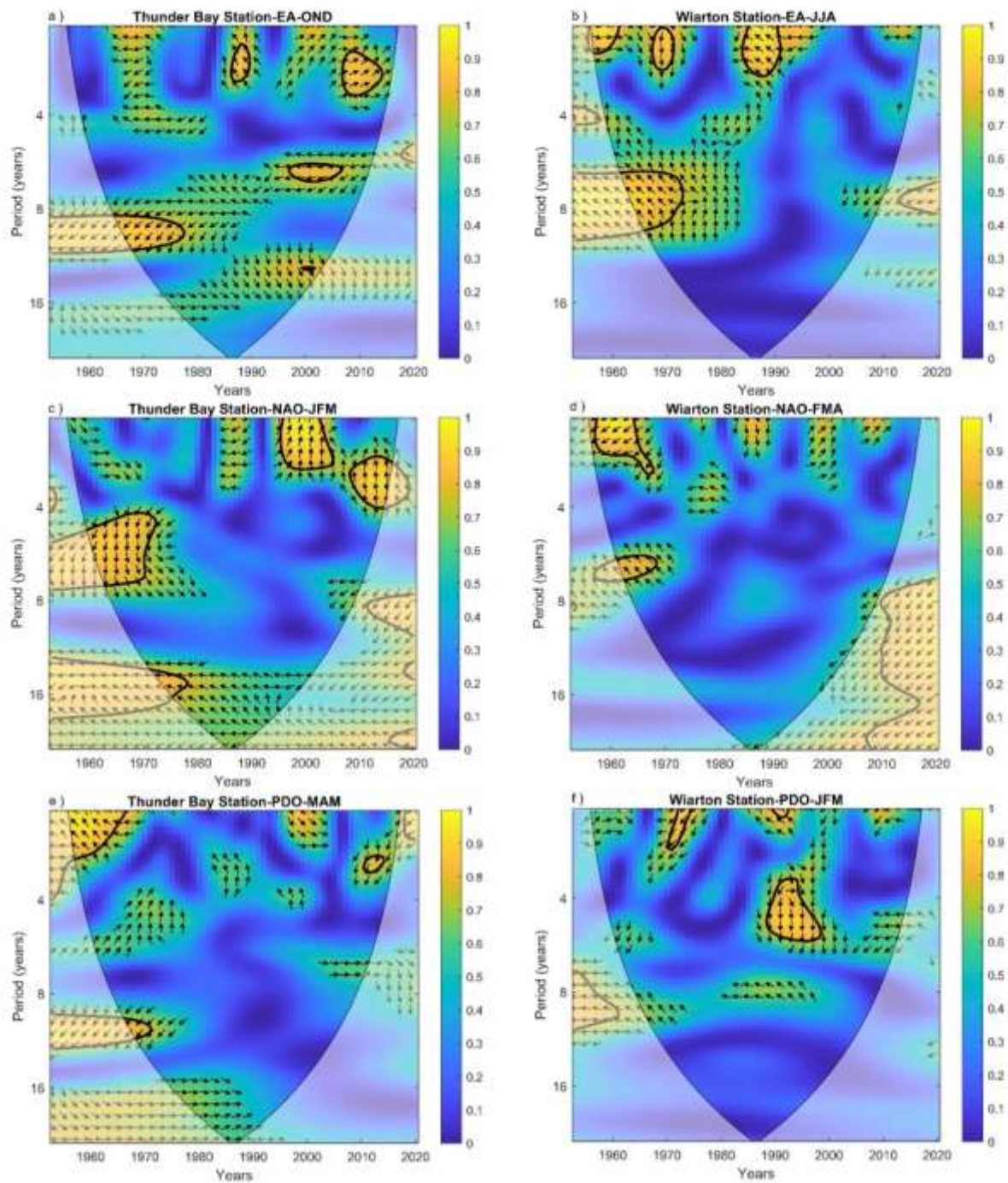


Figure 7: Same as Figure 6 for annual maximum wind speed data.

